NATIONAL ADVISORY COMMITTEE FOR AERONAUTICS

TECHNICAL NOTE 4132

FATIGUE INVESTIGATION OF FULL-SCALE TRANSPORT-AIRPLANE WINGS

VARIABLE-AMPLITUDE TESTS WITH A GUST-LOADS SPECTRUM

By Richard E. Whaley

Langley Aeronautical Laboratory
Langley Field, Va.

Washington
November 1957

NATIONAL ADVISORY COMMITTEE FOR AERONAUTICS

TECHNICAL NOTE 4132

FATIGUE INVESTIGATION OF FULL-SCALE TRANSPORT-AIRPLANE WINGS

VARIABLE-AMPLITUDE TESTS WITH A GUST-LOADS SPECTRUM

By Richard E. Whaley

SUMMARY

This report includes results of simulated flight-history tests which are part of a research program on the fatigue strength of the wings of C-46 airplanes. The tests were conducted by the forced-vibration method, in which a spectrum of loads derived from gust-frequency statistics was used. The results are compared with the previously published results of constant-amplitude fatigue tests.

One crack on each wing grew until the propagation curve indicated that the wing would fail if the test were continued. The cracks grew slowly until a critical percentage of material had failed, after which they grew rapidly. This critical percentage was always fairly small.

The number of crack locations and the number of cracks per wing panel was found to agree better with the higher than with the lower constant-amplitude test results. Most of the cracks that propagated to failure were cracks that did not occur during the majority of the constant-amplitude tests. All cracks grew in a manner similar to the way cracks grew during constant-amplitude tests.

The average crack occurred more than 3.5 times later than the linear-cumulative-damage theory indicated. The first cracks to appear were predicted reasonably well by the theory, but the cracks that propagated to failure initiated about 3 times later than the theory indicated. Final failure of the wings occurred more than 4.5 times later than the theory indicated. The spread for crack initiation was about 5 times as high as the corresponding spread for the constant-amplitude tests.

INTRODUCTION

Few fatigue tests of full-scale airplane wings have been carried out wherein the test loads simulated the flight history for the airplane. Most fatigue tests of full-scale airplane wings have been of a constant-amplitude type in which the results are presented in the form of a load-lifetime relationship. In order to provide a better understanding of the fatigue problems in actual airplanes these constant-amplitude lifetime data must be correlated with the life from actual flight loadings, since airplanes in flight are subjected to a wide variety of loads of various magnitudes and sequence. A related problem is the determination of whether fatigue cracks would occur in the same general locations on airplane wings subjected to flight loadings as they would on wings subjected to constant-amplitude loadings. In order to study the problems a series of simulated flight-history tests were conducted as part of a fatigue research program on C-46 airplane wings.

The results of constant-amplitude fatigue tests on C-46 airplane wings have been reported in references 1 and 2. The present report gives the results of variable-amplitude tests on three complete wings. Included in this report are information on crack initiation and location, the rate and manner of fatigue-crack propagation, and information on the final failure of the wings.

The data gathered from these tests are compared directly with the results of the constant-amplitude tests. The lifetime data are compared with the lifetime data from the constant-amplitude tests by one commonly used method.

SYMBOLS

g	acceleration due to gravity
n/N	cycle ratio (number of cycles applied at a given load level, divided by number of cycles to failure at same load level)
Δn	alternating-load level

EQUIPMENT

Specimen

The general description of the C-46 airplane and a detailed description of the wing structure and its various elements are given in references 1 and 2. Some of the pertinent characteristics of the airplane are given in the following table:

Probable operating gross weight, lb	41,000
Probable level-flight airspeed, fps	281
Wing area, sq ft	1,360
Mean aerodynamic chord, ft	13.688
Slope of the lift curve per radian	4.88

The fatigue specimens, each of which consisted of a center section and two outer panels, were made almost entirely of 2024 aluminum alloy. A cross section of the wing at span station 195, where most of the fatigue cracks occurred, is shown in figure 1.

The wings used in these tests had previously been subjected to from 211 to 1,031 hours of flight service and storage for several years in an open depot. There were no fatigue cracks in the wings due to this short flight history.

Fatigue Machine

The machine used for these tests was specially designed for the application of spectrum-type variable-amplitude loadings. It applied three general kinds of loads to the specimen: the mean or steady-state load, dynamic loads applied with a shaker, and static loads applied with a hydraulic ram. The machine, which was of the forced-vibration type, was symmetrical about the center line of the airplane and is shown in figure 2. The fatigue specimens were mounted in an inverted position in the machine. The wing attachment, tie rods, and shaker unit, which were suspended from the wing, were designed and located in such a way that the mean or steady-state bending moment, shear, and torque at span station 214 were reproduced for the level-flight, low-angle-of-attack condition. This mean load was actually about 1.2g rather than 1 g, which was the mean load produced by the constant-amplitude machine described in reference 3. It was believed that this higher mean load did not have much effect on the life at the low stress levels involved.

The machine could be adjusted quickly to operate at any amplitude up to the allowable limitations of the machine. These limitations were

24,400 pounds of force output and a frequency of 5.33 cycles per second. The machine was driven by two direct-current traction-type electric motors which, with the necessary reduction gears, were located on the laboratory floor at about the middle of each semispan of the wing. A planetary gear box just outboard of the reduction gears was used to drive four shafts which turned four eccentric weights. The force output of the machine was produced by the rotation of the four eccentric weights in the shaker unit, which was suspended from the wing by two tie rods as shown in figure 3.

A large flywheel housing was located between the gear box and the shaker unit as shown in figure 2. An eccentric flywheel on each shaft was statically balanced with the shaker weight on the same shaft for the purpose of reducing the torque in each shaft inboard of this station.

The vertical-force output of the machine was adjusted from the control panel by changing the phase relationship of the top and bottom pairs of shaker weights. This adjustment was made at operating speed by hydraulic operation of a rack and pinion gear at the gear box. An adjustable stop screw limited the travel of the rack to a predetermined value that depended on the amplitude desired.

Static loads were applied by a hydraulic ram fastened to the top of the framework above the shaker unit. This device, shown in figure 3, was used to apply the high loads of the spectrum, which were measured by a load cell at the top of the ram. An automatic coupling device to connect and disconnect the unit from the wing attachment was used so that the total operation could be performed from the control panel.

A system of microswitches and counters was used to count the number of cycles applied at each load level. The microswitch stand can be seen to the left in figure 3. This system is similar to the one used with the constant-amplitude fatigue machine and is described in detail in reference 3.

SIMULATION OF FLIGHT-LOAD HISTORY

Spectrum

In order to provide good correlation between fatigue damage in actual flight and in laboratory tests the loading spectrum to be applied should very nearly duplicate the actual flight-load spectrum. The source of the spectrum chosen for this investigation was the gust-loads data of reference 4. These data were chosen because they were based on a large number of flying hours of several types of transport airplanes and on a wide variety of flight conditions. The spectrum was

composed entirely of gust loads since calculations indicated that loads due to such effects as landings, taxiing, and maneuvers did not contribute significantly to the spectrum. The most severe limits of the data of reference 4 were used. Values of the parameters for the calculation of the spectrum were as follows:

Total flight distance, miles	10^7
Path ratio (average value)	0.1
Density ratio	1.00
Class interval, Δn	0.15
Lowest threshold value, Δn	0.15
Total number of alternating-load levels (chosen in conjunction with the class interval)	16

The calculated loadings that comprised the gust spectrum are given in table 1. The loads in any class interval were applied at the mean of the interval. In order to prevent the application of all the cycles consecutively for any one load level, the total number of loads in each class interval was divided by 100. The result was 100 "sequences" of loads. To minimize the influence of the order of loading on the results, the order in which the load levels were applied in each sequence was determined by the use of a table of random numbers. The first two sequences of the spectrum are shown in table 1, along with the total number of loads that had been applied after each of the two sequences. Of the first 100 sequences, no two were alike in the order of application of the load levels. For each load level with less than 100 cycles in the original spectrum, the cycles were distributed among the 100 sequences as shown in table 2. After the first 100 sequences the spectrum was repeated.

Test Procedure

Variable-amplitude tests were conducted on three complete wings with the fatigue machine and the gust-loads spectrum previously described. Alternating loads lower than ±1 g were applied at frequencies between 2 cps and 4 cps, which was above the wing resonant frequency. The speed of the machine was increased through resonance to the operating speed with zero vertical-force output. After the speed was adjusted the phase relation between the eccentric masses was adjusted to produce the desired amplitude. All loads above an alternating load of ±1 g were applied statically with the static-loading device previously described.

Fatigue cracks were ordinarily discovered when they were about one-quarter of an inch long. Crack initiation is thus defined as

the occurrence of a crack that is one-quarter of an inch long and as deep as the material in which it initiated. This definition is identical with the definition of crack initiation used in discussions of the constant-amplitude tests. The discovery of these small cracks was made possible by the use of bonded wires as crack detectors, supplemented by careful and frequent visual inspections. The use of bonded wires to detect fatigue cracks is described in appendix A of reference 1. Once a crack was discovered, a detailed record of its growth was kept and the growth was correlated with the lifetime. The test was continued until the rate of acceleration of crack growth indicated that the total life of the wing could be estimated with reasonable accuracy.

The close inspection of certain inaccessible areas of these wings was made possible by X-ray photography. The portable X-ray machine, shown in position under the wing in figure 4, had a maximum capacity of 80 kilovolts and 25 milliamperes. The total thickness of aluminum being photographed ranged from 1/8 inch to 5/8 inch, and the exposure times varied up to 8 minutes. Each wing was X-rayed periodically from the time the crack initiated until the end of the test. These X-ray photographs were used to follow the progress of the crack in hidden elements and to detect the initiation of the crack in adjacent hidden elements.

The tube head, containing the X-ray tube and the transformer, was mounted under the wing as close to the compression surface of the wing as possible. The X-ray film was then placed on the tension surface directly over the area to be photographed. The tension surface was about 37 inches from the focal spot of the tube at the wing test section. With this arrangement the compression surface did not show on the photographs. Photographs were taken of crack areas with very little interruption of the test.

RESULTS

Crack Initiation and Classification

All the cracks that were observed are listed in table 3, along with the sequence in which they occurred and the number of cycles equal to or greater than the lowest threshold value of 0.15g. The cracks in the outer panels initiated at seven different locations designated in the plan view of the wing tension surface shown in figure 5. These locations, and one other failure location (VIII), can be described generally as follows:

Location	Description	Span station
I	Vicinity of cutout B	204, 207, 214
II	Corner of cutout F	214
III	Joggle in doubler	195
IV	Corner of cutout H	214
V	Internal reinforcing doubler of cutout C	219
VI	Internal reinforcing doubler of cutout D	219, 228
VII	Internal reinforcing doubler of cutout E	237, 243
VIII	Attach angle bolts	192

Cracks in the center section of the wing were not classified because of their infrequent occurrence.

Location I includes all the cracks that occurred around cutout B because they are very closely related. Similarly, locations VI and VII each include cracks at several screw holes around cutouts D and E.

The failures at location VIII involved the steel bolts which fastened the outer panel of the wing to the center section. This fastening was accomplished by means of an attach angle which ran completely around the surface of the wing at span station 192. (See fig. 5.) During the first two variable-amplitude tests the bolts in the attach angle over the 30-percent-chord spar frequently failed when as few as eight sequences of load had been applied. Some of the bolts about midway between the two spars also failed during these tests. The bolts were always replaced immediately after they failed. The failures stopped when a different type of bolt was used over the 30-percent-chord spar. Because the bolts which failed at location VIII were not part of the outer-panel structure, they are not numbered or listed in table 3.

The cracks in the panels occurred at irregular intervals throughout the lifetime of the specimens. The earliest crack occurred during sequence 6, whereas the latest crack occurred during sequence 193. The spread in lifetime to crack initiation was thus about 32 to 1. The average number of cracks per panel was approximately six.

If only the first crack to appear on each wing is considered, the spread is, of course, much smaller. On one wing it occurred during sequence 6, whereas on another wing it occurred as late as sequence 43. The number of cycles to initiation of these first cracks involves a spread of about 7 to 1.

Four of the six wing panels tested contained cracks at all the locations I to VII. The other two wing panels, considered as a single test specimen, also contained cracks at all seven locations. This consistency in crack location indicates that tests of another specimen would produce cracks in most, if not all, of these locations.

Fatigue-Crack Propagation

In each of the six wing panels tested there was one crack that propagated until it was so large that the wing would have failed if the test had been continued. When these cracks propagated into new structural elements these new cracks were considered part of the original crack. Thus, at the end of the test one crack was large (approximately 20 percent of the chord) and involved several cracked elements. Four of these six cracks originated in location III and the other two originated in location I. (See table 3.)

Cracks did not propagate from locations II, IV, V, VI, and VII. In general, cracks in these locations did not become more than about 1 inch long.

In most of the wings the cracks that propagated were not the first ones to initiate. On one panel, however, the first crack to appear was the one that propagated to final failure. This was crack 17, in the right outer panel of the second specimen tested. In one other panel the crack that propagated was the last one to initiate in that panel. This was crack 41, in the right outer panel of the third specimen. The spread of the number of cycles to initiation of the cracks which propagated was almost 5 to 1.

The crack-propagation curves for each of the cracks that grew are shown in figure 6. In this figure the percentage of tension material failed in a cross section of the wing is plotted against the number of sequences applied. Also shown in this figure are exploded views of a portion of a cross section of the tension surface (from cutout A to cutout F) where the crack growth occurred. Various stages of crack development are indicated by the successive views. The failed portion in each case is represented by the darkened elements. The letters in this figure relate the point on the propagation curve to the particular elements failed and in most cases the letters indicate the start of the crack in a new element.

In each case it can be seen from the curves that the cracks grew slowly until a critical percentage of the material had failed. At this point (defined in ref. 2 as the critical point) the growth of the cracks became very rapid. It can also be seen from figure 6 that the final

failure of the wing could be estimated with reasonable accuracy because of the steep slope of the crack-propagation curve at the cessation of the test. The sequences to final failure listed in table 3 range from 120 to 218, a spread of less than 2 to 1.

The data of figure 6 show that the critical point always occurred at about 95 percent of the lifetime. The critical percentages listed in table 3 vary from 5.5 to 13.5 percent. Thus, in each case the critical point is reached when less than 14 percent of the total tension cross-sectional area has failed.

The portions of the total lifetime remaining after the cracks reached a value of 1 percent of the total tension cross-sectional area are listed in table 3. From these values it can be seen that in every case the crack was present in the panel for at least 29 percent of the total lifetime.

The X-ray equipment described earlier was used extensively to follow the progress of the cracks through the structure. Location III, which consisted of three thicknesses of sheet material and one leg of the attach angle, was photographed most. The progress of a typical crack in this location can be seen in figure 6(d). The crack was usually detected by a crack-detector wire in the external doubler plate over the 30-percent-chord spar. Periodic X-ray photographs were then made to determine the inception and progress of the crack in the middle doubler plates and the skin. A series of X-ray photographs of this area, showing the progress of the crack forward of the 30-percent-chord spar, can be seen in figure 7.

The use of X-ray photographs was also required for location I. The progress of a crack in this area can be seen in figure 6(c). The inception of the crack in the heavy T-stiffener forward of the cutout in this area was hidden by the several thicknesses of skin and doubler plates. An X-ray photograph of a crack in this stiffener can be seen in figure 8.

Final Failure

As mentioned previously, the final-failure points were estimated from the propagation curves. These points are listed in table 3 and indicate a spread in lifetime of less than 2 to 1. This is a much smaller spread than that for initiation of the first cracks in each wing (about 7 to 1) and of the cracks that propagated (about 5 to 1).

In no case were the wings intentionally loaded to final failure during the fatigue test. The right wing of the second specimen failed completely during the fatigue test at a total load of about 2.90g. Inspection of the failed elements after the test did not reveal the

presence of a larger crack than had been observed prior to the failure and shown in figure 6(c). On the basis of the information in reference 2, this panel failed at a load that was slightly less than the expected failing load.

COMPARISON WITH CONSTANT-AMPLITUDE RESULTS

Crack Initiation and Classification

A comparison was made between the locations where cracks occurred during the variable-amplitude tests and the locations where cracks occurred during the constant-amplitude tests (given in ref. 1). In reference 1 the cracks are not classified according to their specific locations, as in the present report, but they can easily be so classified from the description of each crack. In this reference, crack initiation was reported at one location on the outer panel that does not appear in the present report, that labeled "Edge of external doubler plate, station 207." In the variable-amplitude tests these cracks were included in location I because when they did occur they had always started first at some other point in the vicinity of cutout B.

The number of locations at which cracks were observed during these two types of tests are shown in figure 9. The number of locations increased with increasing load level, and there were as many crack locations in the variable-amplitude tests as in any of the constant-amplitude tests. Most of the locations at which cracks were observed during the constant-amplitude tests were repeated during the variable-amplitude tests. There were, however, no new crack locations.

The same general comparison can be made for the bolt failures of location VIII. These serious bolt failures occurred during the high constant-amplitude tests at the 1.000g level, once during the test of each specimen. The failures occurred once during one of the 0.625g tests. That these bolt locations are a potential source of failure was not revealed during any of the lower constant-amplitude tests or during most of the intermediate constant-amplitude tests.

The average number of cracks per panel was also compared with the results for the constant-amplitude tests. The data from reference 1, shown in figure 10, indicate that the number of cracks per panel increased with increasing load level. The number of cracks per panel during the variable-amplitude tests was larger than for any of the load levels of the constant-amplitude tests. The results of the comparisons indicate that the frequency of occurrence of fatigue cracks during the variable-amplitude tests agrees better with the higher than with the lower load levels of the constant-amplitude tests. They also indicate that any

constant-amplitude test, particularly one at a low level, may not reveal the location and frequency of all cracks that may occur during variable-amplitude loading.

Fatigue-Crack Propagation

A comparison was made between the rate and manner of fatigue-crack propagation during these tests and the constant-amplitude results in reference 2. As stated previously, four of the six cracks that propagated to failure in the variable-amplitude tests originated in location III and the other two originated in location I. These constitute two of the three locations from which cracks propagated to failure during the constant-amplitude tests. However, a crack propagated to failure from location III in only one of the eighteen wings of the constant-amplitude tests. This crack occurred during a high constant-amplitude test. Thus it appears that any one constant-amplitude test may not reveal the location of the cracks that will propagate to failure in a wing subjected to flight loadings.

No cracks propagated to failure from location II in the variable-amplitude tests, but three cracks propagated from this point during the higher constant-amplitude tests. Thus it appears that a crack that does not look serious during the variable-amplitude tests is more serious during high constant-amplitude tests.

In figure 11 the propagation curve for a variable-amplitude test is compared with the propagation curves for several load levels of the constant-amplitude tests. The abscissa in this figure is the number of cycles applied, expressed as a percentage of the cycles to complete wing failure as estimated from the propagation curves of figure 6 and reference 2. It can be seen that the propagation curves from both investigations have about the same general shape in that a long period of slow crack growth precedes rapid growth. There are two general types of curves shown in this figure, those that grow slowly up to the critical point with no serious change in slope and one that has a sudden increase in slope at about 80 percent of the lifetime. These two types are associated with the crack location rather than the load level, and both types occurred during the variable-amplitude tests, as shown in figure 6.

The results of the constant-amplitude tests indicated that, although there was scatter, the critical percentage varied with the load level. This trend is shown by the solid line in figure 12. Some of the scatter is attributable to the failure location. The critical percentages for the location I failures are generally higher than the critical percentages for the location III failures. Also shown in this figure are the critical percentages from the variable-amplitude data. These also have a

great deal of scatter; they cannot be associated with any one particular load level but vary anywhere between the high constant-amplitude results and the low constant-amplitude results. The critical percentages from the location I failures are again higher than the critical percentages from the location III failures.

Lifetime Comparison

A comparison of the lifetime data for the variable-amplitude and constant-amplitude tests involves the use of the load-lifetime relationship. Figure 13 shows the load-lifetime curves from the constant-amplitude tests, with the alternating load level expressed as a function of the number of cycles. These curves, for the most part, were plotted directly from the data of reference 1. They were modified, however, by results given in table 4 for a constant-amplitude test not reported in reference 1. The curves include all the center-section data but they would not be changed appreciably if these data were omitted.

Curve C is a numerically averaged curve of crack initiation for all cracks. It is also the numerically averaged curve of crack initiation for the cracks that propagated to final failure. Curve F is a numerically averaged curve for the first crack to appear on each wing. Curves A and B represent the limits within which 95 percent of all cracks could be expected to occur at each level, as determined by statistical methods. These curves represent a spread of about 6 to 1. Curve E is a numerically averaged curve through the final-failure data. Curves B and D represent the limits of the scatter for final failure of the wings.

It is possible, with the present data, to make many different comparisons between the variable-amplitude lifetime data and the constant-amplitude lifetime data. The comparisons which are discussed were chosen because they seem to be of the most general interest at this time. There are also a number of methods for relating the two sets of data. The commonly used linear-cumulative-damage theory (ref. 5) is discussed in this paper. On the basis of this theory, the summation of the cycle ratios should equal 1 at failure, or $\sum \frac{n}{N} = 1$ where n is the number of cycles applied at any given load level in the spectrum loading and N is the number of cycles to failure at the same load level.

Crack initiation.- For each crack, the summation of the cycle ratios based on each of the three load-lifetime curves A, B, and C is listed in table 5. The summation of the cycle ratios for the first cracks to appear on each wing, based on curve F, is also listed. From this table

it can be seen that the values of $\sum \frac{n}{N}$ as computed with the average curve C were almost always greater than 1 for all the cracks. The average value of $\sum \frac{n}{N}$ was 3.52, which means that the average life to the initiation of all the cracks was more than 3.5 times that predicted by the cumulative-damage theory. This does not mean, however, that the first cracks appeared 3.5 times later than would be predicted by this theory. The average value of $\sum \frac{n}{N}$ for the first crack to appear on each wing, based on curve F, was 1.45. This means that on an average the life to the initiation of the first crack was close to the predicted value.

For the six cracks that propagated to final failure, the average value of $\sum \frac{n}{N}$ based on curve C and shown in table 4 was 2.87. Thus, these cracks appeared much later than would be predicted. One (crack 17), however, appeared only slightly later than would be predicted, as evidenced by the value of $\sum \frac{n}{N} = 1.09$.

Spread.- The spread in lifetime to crack initiation for the variable-amplitude data (32 to 1) was 5 times that for the constant-amplitude data (6 to 1). This is evidenced by the fact that the lifetime to the initiation of the first cracks was about the same as the predicted value, but the lifetimes to the initiation of the cracks that propagated to final failure and the initiation of the average crack were much greater than the predicted values.

Final failure.- In five of the six wing panels tested, more cycles were applied at each of the three lowest load levels than were required to cause failure during constant-amplitude tests at those levels. The values of $\sum \frac{n}{N}$ for the final failure of each outer panel are presented in table 5. The average value of $\sum \frac{n}{N}$, based on the average curve E, was 4.81, which means that the wings lasted more than 4.8 times the predicted lifetime. Examination of the values of $\sum \frac{n}{N}$ for final failure,

based on the limits of the scatter of the constant-amplitude data, shows that the lowest value of $\sum \frac{n}{N}$ for the high end of the scatter (curve B) was 2.75. This means that any calculation based on the cumulative-damage theory and the constant-amplitude results would have underestimated the fatigue life. The spread in fatigue life was only slightly greater than the spread from the constant-amplitude tests.

A possible reason for the high average values of $\sum \frac{n}{N}$ may be a beneficial effect of the infrequent high loads. Reference 6 shows that periodically loading a structure to 50 percent of the ultimate strength during a constant-amplitude test increased the lifetime by a factor of about 5. The fatigue loading in reference 6 was 25 ± 7.5 percent of the ultimate strength. The high loads in the spectrum used here were about 50 percent of the ultimate strength of the tension surface of the wing as calculated in reference 2.

In figure 14 the cycle ratio $\frac{n}{N}$ is plotted against the load level of the spectrum for a typical crack. The figure shows that the highest loads were applied so infrequently that their cycle ratios were negligible compared with the cycle ratios for the lower load levels. The periodic application of these high loads may have had the same effect as the periodic high loading reported in reference 6. This same effect may account for the higher spread in the variable-amplitude lifetimes than in constant-amplitude lifetimes.

A closer examination of figure 14 shows that, according to the linear-cumulative-damage theory, most of the damage was caused by loads between about 0.3g and 0.45g, as indicated by the high, sharp peak. This concentration of damage in a narrow band has generally led to the assumption that other load levels have very little effect on the damage, and thus the damage could be assessed with very little error by considering one small range of loads. Further simplification would result in a constant-amplitude test at a low load level. This report shows that the theory of linear cumulative damage results in an underestimated life. Further, as outlined in the section entitled "Results," a constant-amplitude test at this low load level may not reveal the locations of all the cracks, particularly the ones that propagate and ultimately cause failure of the wing.

CONCLUSIONS

Variable-amplitude fatigue tests have been conducted on three complete wing structures by applying a loading spectrum calculated from gust-frequency statistics. From the results of these tests and the results of constant-amplitude tests published previously, the following conclusions were reached:

1. The number of crack locations and the total number of cracks per wing were found to agree better with the higher than with the lower constant-amplitude results. Although no new crack locations were found, variable-amplitude tests tended to produce more crack locations than were found at any one constant-amplitude load level.

2. Most of the cracks that propagated to failure during variable-amplitude loading were cracks that appeared very infrequently, and only at high amplitudes, during the constant-amplitude tests.

3. Cracks propagated in a manner similar to that in which they propagated during constant-amplitude loading. The cracks grew slowly until about 95 percent of the load sequences had been applied, after which they grew rapidly. The critical percentage of material that had failed when cracks began to grow rapidly had too much scatter to be associated with any of the constant-amplitude results.

4. If all cracks are considered, the average crack occurred more than 3.5 times later than predicted by the linear-cumulative-damage theory. The cracks that propagated to final failure occurred about 3 times later than predicted by this theory, but the occurrence of the first crack on each wing was predicted reasonably well by this theory.

5. The spread in lifetime to crack initiation, for all the cracks, was about 5 times as large in the variable-amplitude tests as in the constant-amplitude tests.

6. The linear-cumulative-damage theory greatly underestimated the final life. In five of the six wing panels tested, more cycles were applied at each of the three lowest load levels than were required to cause failure during constant-amplitude tests at those levels.

Langley Aeronautical Laboratory,
National Advisory Committee for Aeronautics,
Langley Field, Va., August 13, 1957.

REFERENCES

1. McGuigan, M. J., Jr., Bryan, D. F., and Whaley, R. E.: Fatigue Investigation of Full-Scale Transport-Airplane Wings - Summary of Constant-Amplitude Tests Through 1953. NACA TN 3190, 1954.

2. Whaley, Richard E., McGuigan, M. J., Jr., and Bryan, D. F.: Fatigue-Crack-Propagation and Residual-Static-Strength Results on Full-Scale Transport-Airplane Wings. NACA TN 3847, 1956.

3. McGuigan, M. James, Jr.: Interim Report on a Fatigue Investigation of a Full-Scale Transport Aircraft Wing Structure. NACA TN 2920, 1953.

4. Rhode, Richard V., and Donely, Philip: Frequency of Occurrence of Atmospheric Gusts and of Related Loads on Airplane Structures. NACA WR L-121, 1944. (Formerly NACA ARR L4121.)

5. Miner, Milton A.: Cumulative Damage in Fatigue. Jour. Appl. Mech., vol. 12, no. 3, Sept. 1945, pp. A-159 - A-164.

6. Raithby, K. D., and Longson, Jennifer: Some Fatigue Characteristics of a Two Spar Light Alloy Structure (Meteor 4 Tailplane). Rep. No. Structures 195, British R.A.E., Jan. 1956.

TABLE 1

LOADING SPECTRUM

Threshold, Δn	Summation of cycles	Load level, Δn	Cycles in class interval
0.15	5,967,000	0.225	3,931,200
.30	2,035,800	.375	1,544,400
.45	491,400	.525	351,000
.60	140,400	.675	106,700
.75	33,696	.825	23,510
.90	10,179	.975	7,301
1.05	2,878	1.125	2,036
1.20	842	1.275	586
1.35	260	1.425	148
1.50	112	1.575	69
1.65	43	1.725	19
1.80	24	1.875	12
1.95	12	2.025	6
2.10	6	2.175	2
2.25	4	2.325	2
2.40	2	2.475	1
2.55	1		

First sequence	
Load level, Δn	Cycles in class interval
0.525	3,510
2.475	0
1.875	0
2.325	0
.675	1,067
2.025	0
.975	73
1.575	1
1.725	0
1.275	6
2.175	0
1.125	20
1.425	1
.825	235
.225	39,312
.375	15,444

Load level, Δn	Total cycles
0.225	39,312
.375	15,444
.525	3,510
.675	1,067
.825	235
.975	73
1.125	20
1.275	6
1.425	1
1.575	1
1.725	0
1.875	0
2.025	0
2.175	0
2.325	0
2.475	0
Summation of cycles	59,669

Second sequence	
Load level, Δn	Cycles in class interval
1.725	0
2.175	0
.825	236
1.425	1
1.275	5
1.575	1
1.125	20
2.475	0
.375	15,444
.225	39,312
.675	1,067
.525	3,510
.975	73
2.025	0
2.325	0
1.875	1

Load level, Δn	Total cycles
0.225	78,624
.375	30,888
.525	7,020
.675	2,134
.825	471
.975	146
1.125	40
1.275	11
1.425	2
1.575	2
1.725	0
1.875	1
2.025	0
2.175	0
2.325	0
2.475	0
Summation of cycles	119,339

TABLE 2

RANDOMIZED LOADS GREATER THAN $\Delta n = 1.5$

Sequence	Load level, Δn						
	1.575	1.725	1.875	2.025	2.175	2.325	2.475
1	X						
2	X		X				
3	X		X				
4	X			X			
5	X						
6					X		
7	X						
8	X						
9	X						
10	X						
11							
12	X						
13	X						
14		X					
15							
16							
17	X		X				
18	X						
19	X		X				
20				X			
21	X						
22	X	X					
23							
24							
25	X						
26	X						
27	X						
28							
29	X	X				X	
30	X						
31							
32							
33			X				
34							
35	X	X					
36	X						
37							
38	X						
39	X	X					
40		X					
41	X		X				
42							
43	X						
44					X		
45	X						
46	X						
47	X						
48							
49	X						
50	X	X					

Sequence	Load level, Δn						
	1.575	1.725	1.875	2.025	2.175	2.325	2.475
51	X						
52	X	X					
53	X		X				
54	X						
55	X		X	X			
56							
57		X					
58	X						
59							
60	X			X			
61	X	X					
62							
63	X						
64	X						
65							
66	X						
67		X					
68	X						
69	X						
70	X						
71	X	X					
72	X	X					
73				X			
74	X	X					
75	X						
76							
77	X						
78	X						X
79	X	X					
80	X						
81	X						
82		X					
83	X						
84	X						
85	X		X				
86	X		X				
87						X	
88	X	X					
89			X				
90	X						
91	X						
92	X						
93	X						
94				X			
95	X						
96	X		X				
97	X	X					
98	X						
99	X	X					
100							

TABLE 3

SUMMARY OF DATA

(a) Specimen 1

Crack	Description (a)	Location	Sequence at crack initiation	Total cycles to crack initiation	Sequence at 1 percent failure	Sequence at estimated final failure	Lifetime after 1 percent failure, percent	Area failed at critical point, percent
1	Corner of inspection cut-out F, station 214 (L, OP)	II	23	1,352,062				
2	Internal reinforcing doubler plate of inspection cut-out E, station 239 (R, OP)	VII	23	1,352,062				
3	Corner of inspection cut-out B, station 204 (R, OP)	I	28	1,670,790				
4	Internal reinforcing doubler plate of inspection cut-out C, station 228 (R, OP)	V	37	2,168,187				
5	Internal reinforcing doubler plate of inspection cut-out D, station 228 (L, OP)	VI	37	2,168,187				
6	Internal reinforcing doubler plate of inspection cut-out E, station 239 (L, OP)	VII	58	3,460,601				
7	Corner of inspection cut-out H, station 214 (R, OP)	IV	59	3,486,779				
8	Corner of inspection cut-out H, station 214 (L, OP)	IV	59	3,486,779				
9	Corner of inspection cut-out F, station 214 (R, OP)	II	60	3,580,215				
10	Joggle in external doubler plate, station 195 (L, OP)	III	60	3,580,215	63	150	58.0	5.5
11	Joggle in external doubler plate, station 195 (R, OP)	III	68	4,057,571	79	145	45.5	6.0
12	Outboard juncture of wing and nacelle, station 180 (R, CS)		96	5,712,808				
13	Outboard juncture of wing and nacelle, station 180 (L, CS)		111	6,619,644				
14	Edge of inspection cut-out B, station 207 (L, OP)	I	113	6,722,387				
15	Internal reinforcing doubler plate of inspection cut-out C, station 228 (L, OP)	V	121	7,199,895				
16	Internal reinforcing doubler plate of inspection cut-out D, station 228 (R, OP)	VI	125	7,458,555				

[a]Letters in parentheses refer to the following: L, left wing; R, right wing; OP, outer panel; CS, center section.

TABLE 3.- Continued

SUMMARY OF DATA

(b) Specimen 2

Crack	Description (a)	Location	Sequence at crack initiation	Total cycles to crack initiation	Sequence at 1 percent failure	Sequence at estimated final failure	Lifetime after 1 percent failure, percent	Area failed at critical point, percent
17	Corner of inspection cut-out B, station 214 (R, OP)	I	24	1,417,842	107	173	38.1	13.0
18	Internal reinforcing doubler plate of inspection cut-out E, station 239 (L, OP)	VII	28	1,670,741				
19	Corner of inspection cut-out B, station 214 (L, OP)	I	32	1,865,477				
20	Joggle in external doubler plate, station 195 (L, OP)	III	60	3,524,057	65	120	45.8	8.0
21	Corner of inspection cut-out H, station 214 (L, OP)	IV	60	3,563,455				
22	Internal reinforcing doubler plate of inspection cut-out D, station 228 (R, OP)	VI	77	4,552,036				
23	Internal reinforcing doubler plate of inspection cut-out C, station 228 (L, OP)	V	86	5,091,876				
24	Joggle in external doubler plate, station 195 (R, OP)	III	95	5,668,612				
25	Riveted tension joint, station 32 (L, CS)		127	7,539,158				
26	Corner of inspection cut-out F, station 214 (R, OP)	II	134	8,054,137				
27	Corner of inspection cut-out H, station 214 (R, OP)	IV	146	8,711,839				

[a]Letters in parentheses refer to the following: L, left wing; R, right wing; OP, outer panel; CS, center section.

TABLE 3.- Concluded

SUMMARY OF DATA

(c) Specimen 3

Crack	Description (a)	Location	Sequence at crack initiation	Total cycles to crack initiation	Sequence at 1 percent failure	Sequence at estimated final failure	Lifetime after 1 percent failure, percent	Area failed at critical point, percent
28	Internal reinforcing doubler plate of inspection cut-out D, station 228 (L, OP)	VI	6	354,280				
29	Outboard juncture of wing and nacelle, station 180 (R, CS)		17	970,302				
30	Internal reinforcing doubler plate of inspection cut-out E, station 239 (L, OP)	VII	21	1,253,114				
31	Internal reinforcing doubler plate of inspection cut-out D, station 228 (R, OP)	VI	43	2,506,842				
32	Corner of inspection cut-out B, station 214 (R, OP)	I	47	2,749,766				
33	Corner of inspection cut-cut B, station 204 (L, OP)	I	47	2,789,031	128	219	41.5	13.5
34	Internal reinforcing doubler plate of inspection cut-out E, station 239 (R, OP)	VII	65	3,878,514				
35	Corner of inspection cut-out H, station 214 (L, OP)	IV	75	4,475,342				
36	Internal reinforcing doubler plate of inspection cut-out C, station 228 (L, OP)	V	78	4,614,581				
37	Corner of inspection cut-out H, station 214 (R, OP)	IV	78	4,614,581				
38	Corner of inspection cut-out F, station 214 (R, OP)	II	82	4,893,706				
39	Internal reinforcing doubler plate of inspection cut-out C, station 228 (R, OP)	V	94	5,608,367				
40	Corner of inspection cut-out F, station 214 (L, OP)	II	107	6,405,124				
41	Joggle in external doubler plate, station 195 (R, OP)	III	116	6,906,293	130	183	29.0	8.5
42	Riveted tension joint, station 32 (L, CS)		125	7,458,868				
43	Joggle in external doubler plate, station 189 (L, CS)		128	7,583,791				
44	Outboard juncture of wing and nacelle, station 180 (L, CS)		140	8,313,725				
45	Joggle in external doubler plate, station 189 (R, CS)		150	8,890,964				
46	Joggle in external doubler plate, station 195 (L, OP)	III	193	11,516,285				

[a]Letters in parentheses refer to the following: L, left wing; R, right wing; OP, outer panel; CS, center section.

TABLE 4

CONSTANT-AMPLITUDE DATA[a]

$[\Delta n = 0.250]$

Crack	Description (b)	Location	Measured stress, lb/sq in. (c)		Cycles to crack initiation	Cycles to estimated final failure of wing
			1 g mean	Alternating		
1	Edge of external doubler plate, station 207 (L,OP, 9)	I	9,640	2,410	2,401,000	4,174,000
2	Edge of external doubler plate, station 207 (R,OP, 9)	I	9,640	2,410	3,187,000	5,000,000
3	Riveted shear joint, station 120 (L, CS, 9)		8,590	2,150	3,400,000	
4	Outboard juncture of wing and nacelle, station 180 (L, CS, 9)		7,190	1,800	4,174,000	

[a]These data supplement the data from reference 1 used in this report.

[b]Letters in parentheses refer to the following: L, left wing; R, right wing; CS, center section; OP, outer panel. Numbers in parentheses refer to the order in which wing panels were tested during constant-amplitude tests.

[c]Nominal stress near point of failure.

TABLE 5

LIFETIMES BASED ON CUMULATIVE-DAMAGE THEORY

Crack	Crack initiation					Final failure of wing			
	Sequence at crack initiation	$\sum \frac{n}{N}$ based on -				Sequence at final failure of wing	$\sum \frac{n}{N}$ based on -		
		Curve A	Curve B	Curve C	Curve F		Curve D	Curve B	Curve E
28	6	0.72	0.13	0.27	0.35				
29	17	2.04	.38	.76					
30	21	2.62	.48	.97					
1	23	2.76	.51	1.03	1.34				
2	23	2.76	.51	1.03	1.34				
17	24	2.93	.55	1.09	1.43	174	6.24	4.00	5.07
18	28	3.48	.64	1.29	1.69				
3	28	3.48	.64	1.29					
19	32	3.91	.71	1.45					
4	37	4.57	.84	1.69					
5	37	4.57	.84	1.69					
31	43	5.22	.97	1.94	2.53				
32	47	5.77	1.06	2.14					
33	47	5.79	1.06	2.15		218	7.85	5.03	6.37
6	58	7.21	1.33	2.68					
7	59	7.25	1.34	2.69					
8	59	7.25	1.34	2.69					
20	60	7.37	1.36	2.73		120	4.30	2.75	3.49
21	60	7.39	1.37	2.75					
9	60	7.46	1.38	2.77					
10	60	7.46	1.38	2.77		150	5.37	3.45	4.36
34	65	8.09	1.50	3.00					
11	68	8.46	1.57	3.14		145	5.17	3.32	4.20
35	75	9.33	1.73	3.46					
22	77	9.53	1.76	3.54					
36	78	9.66	1.79	3.58					
37	78	9.66	1.79	3.58					
38	82	10.21	1.89	3.79					
23	86	10.66	1.97	3.95					
39	94	11.69	2.16	4.34					
24	95	11.82	2.19	4.39					
12	96	11.89	2.20	4.41					
40	107	13.42	2.48	4.93					
13	111	13.77	2.55	5.11					
14	113	13.96	2.58	5.18					
41	116	14.38	2.66	5.34		183	6.59	4.24	5.35
15	121	19.99	2.77	5.57					
16	125	15.54	2.88	5.77					
42	125	15.55	2.88	5.77					
25	127	15.78	2.98	5.86					
43	128	15.82	2.93	5.87					
26	134	16.80	3.11	6.24					
44	140	17.38	3.22	6.46					
27	146	18.16	3.36	6.74					
45	150	18.54	3.43	6.88					
46	193	23.41	4.44	8.91					
Average				3.52	1.45				4.81

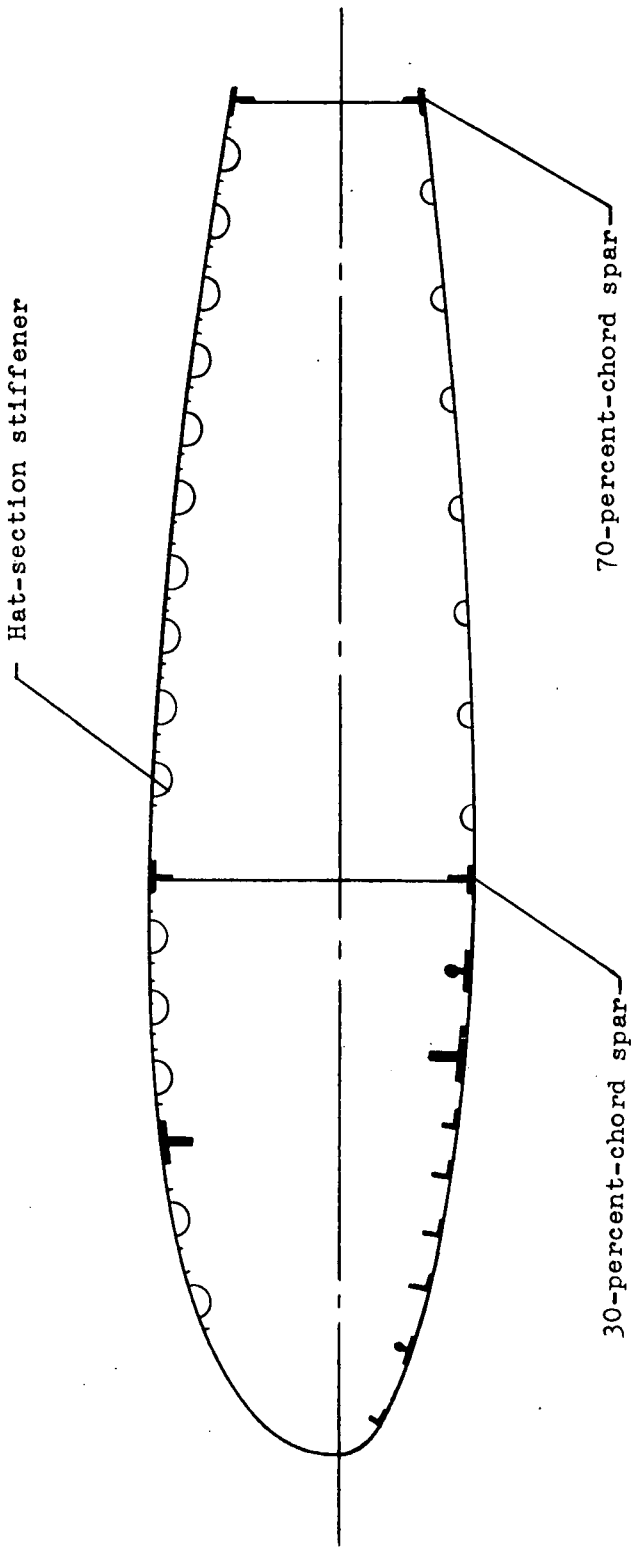

Figure 1.- General arrangement of section of outer panel at station 195.

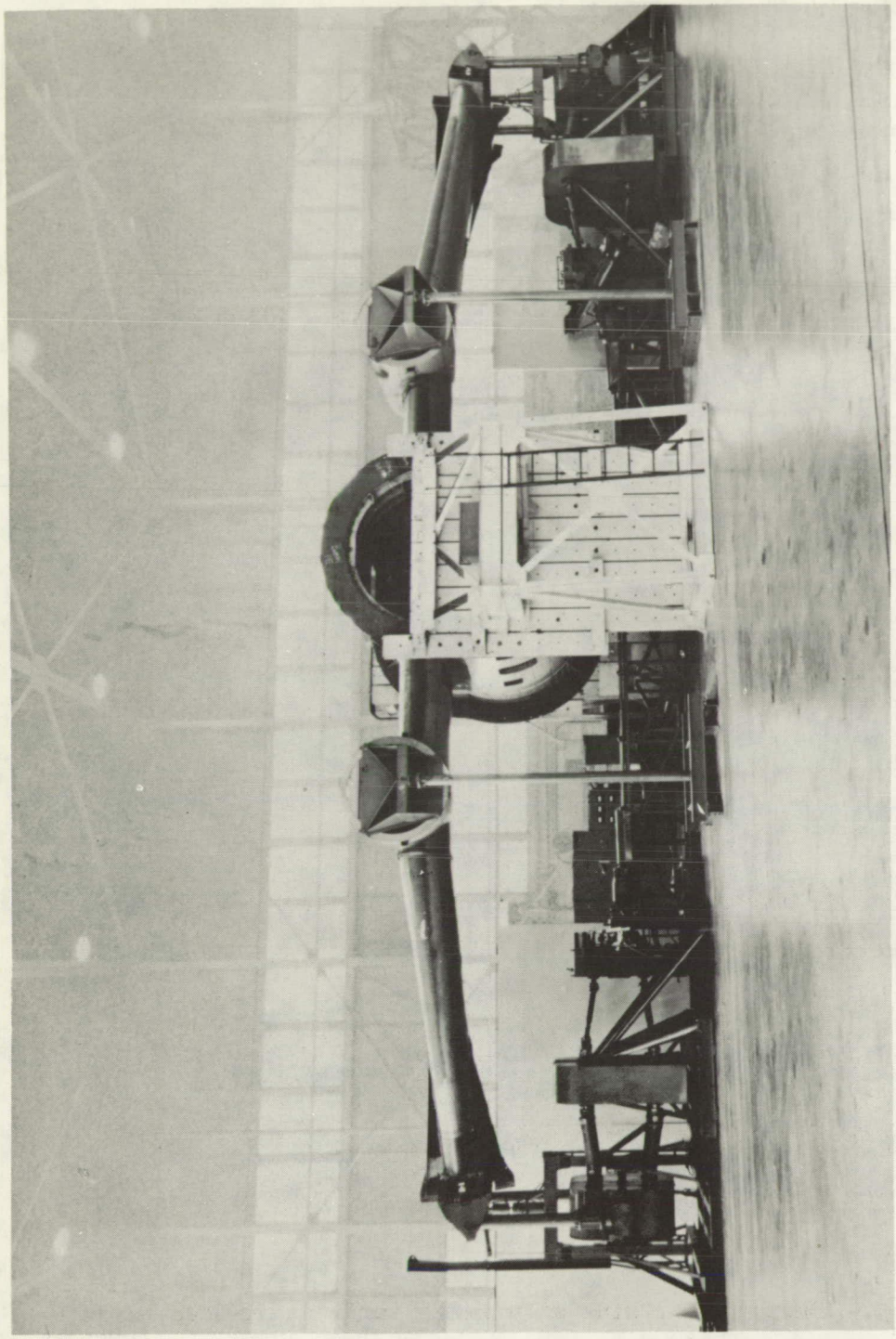

Figure 2.- General view of wing mounted in variable-amplitude fatigue machine. L-57-479.1

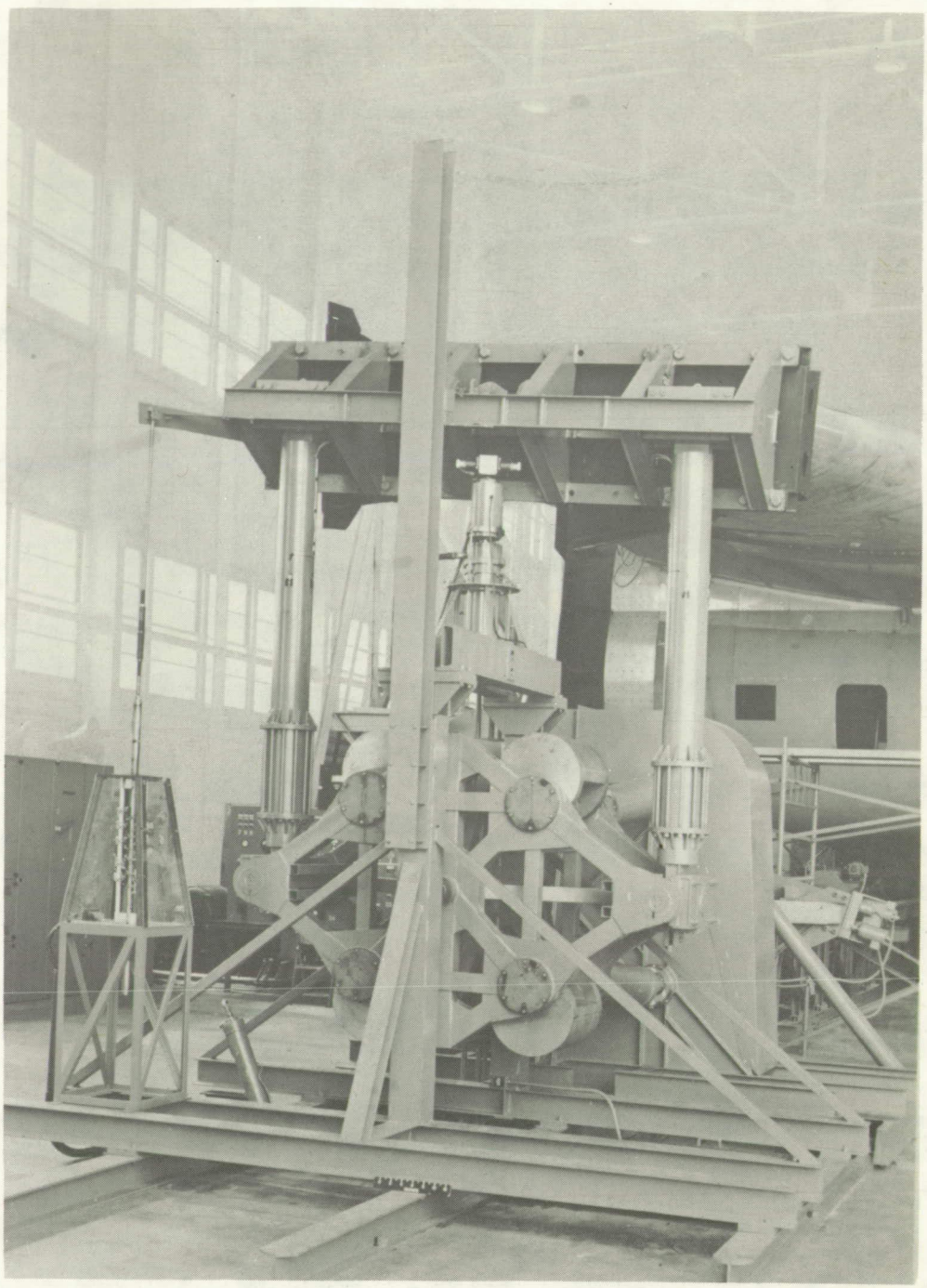

L-85912.1

Figure 3.- Shaker unit, wing attachment, and static-loading rig.

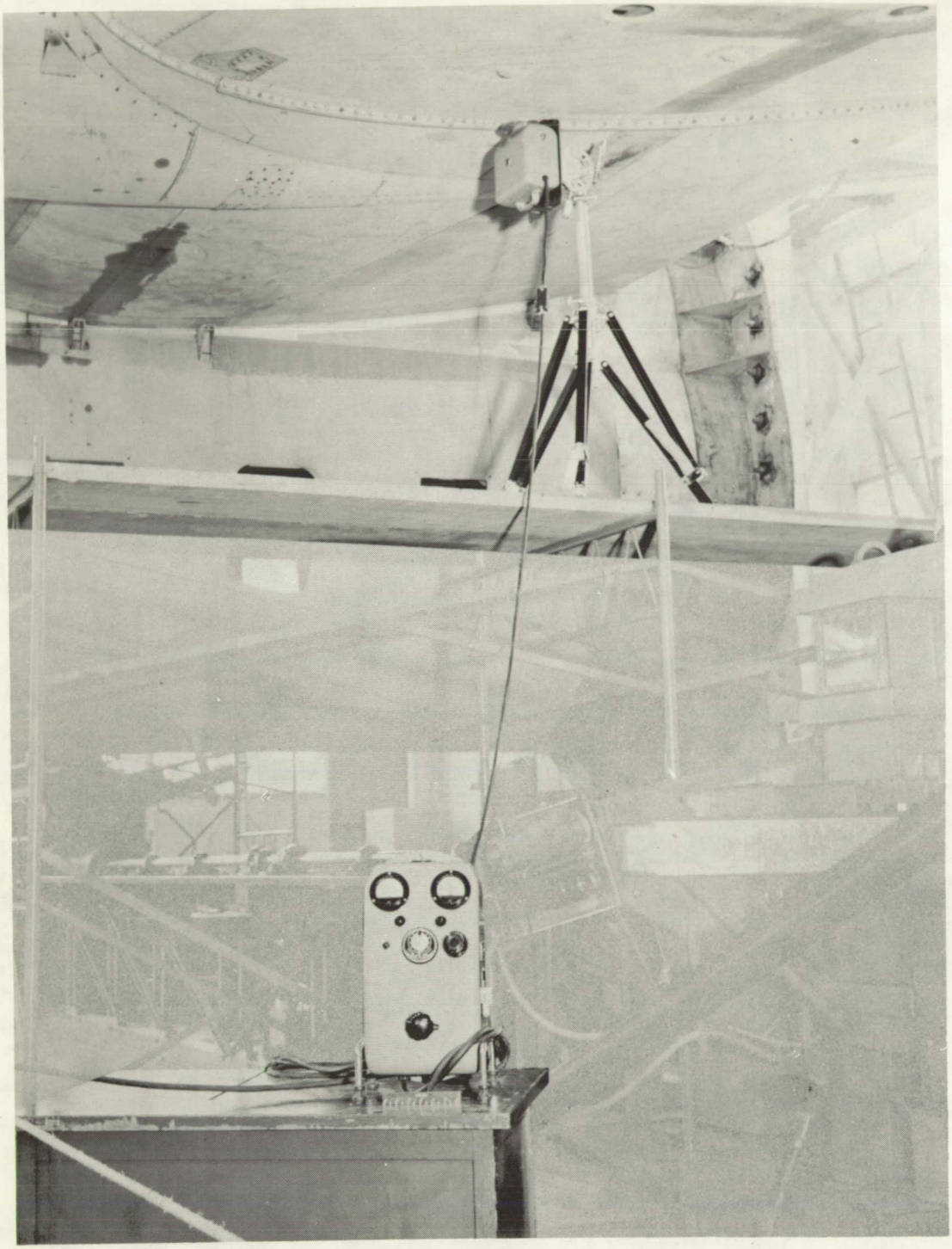

Figure 4.- X-ray machine mounted under wing. L-96395.1

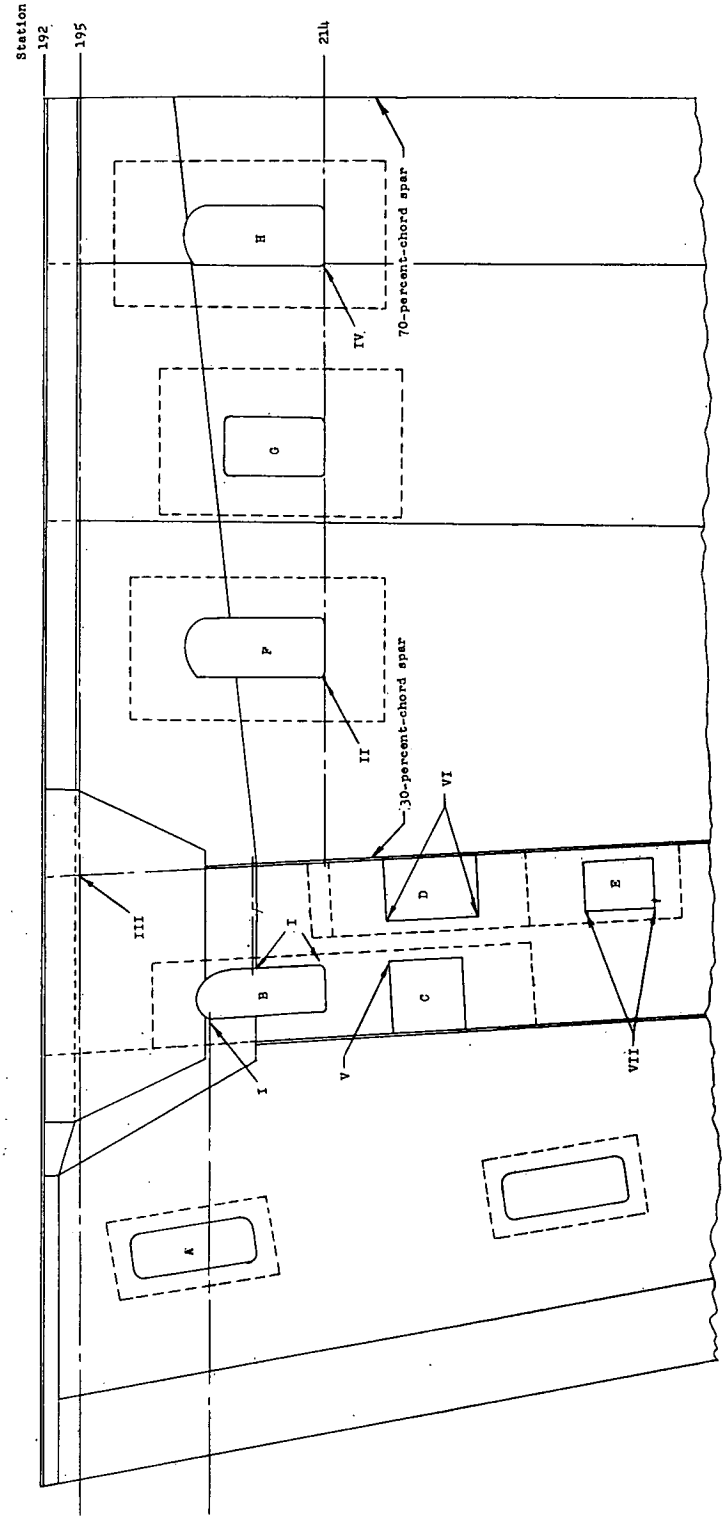

Figure 5.- Details of wing surface. Letters designate inspection cutouts; Roman numerals designate locations at which cracks initiated.

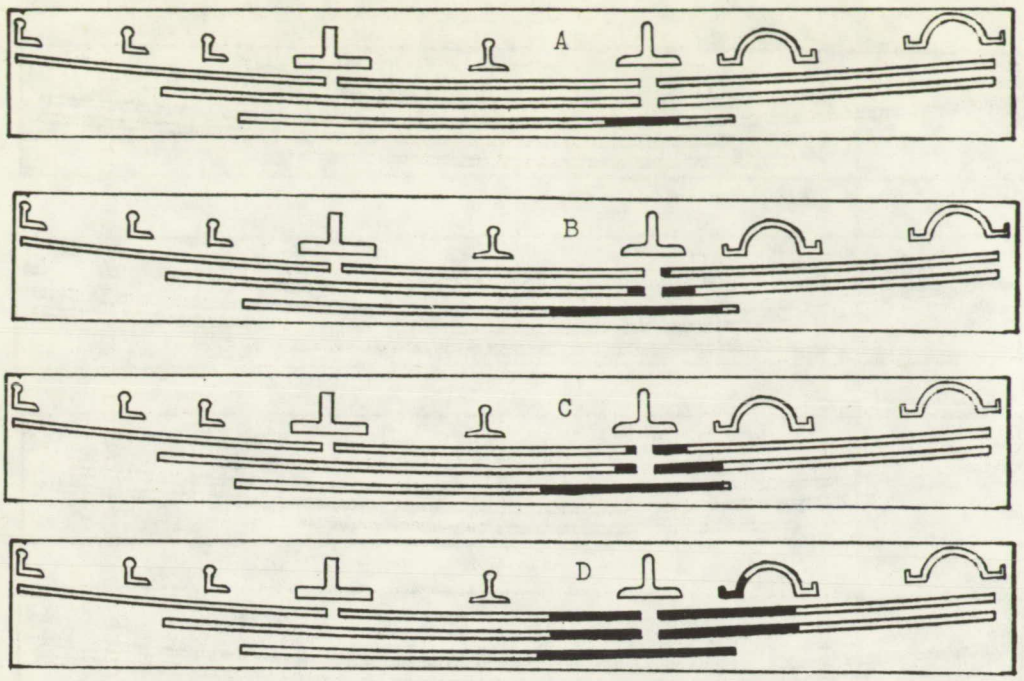

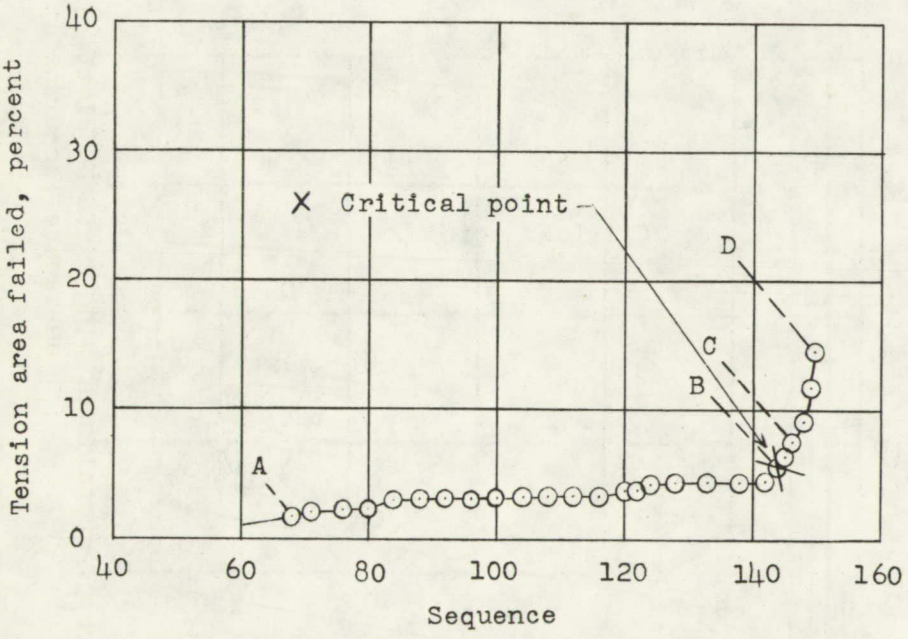

(a) Crack 10; location III.

Figure 6.- Crack propagation through wings.

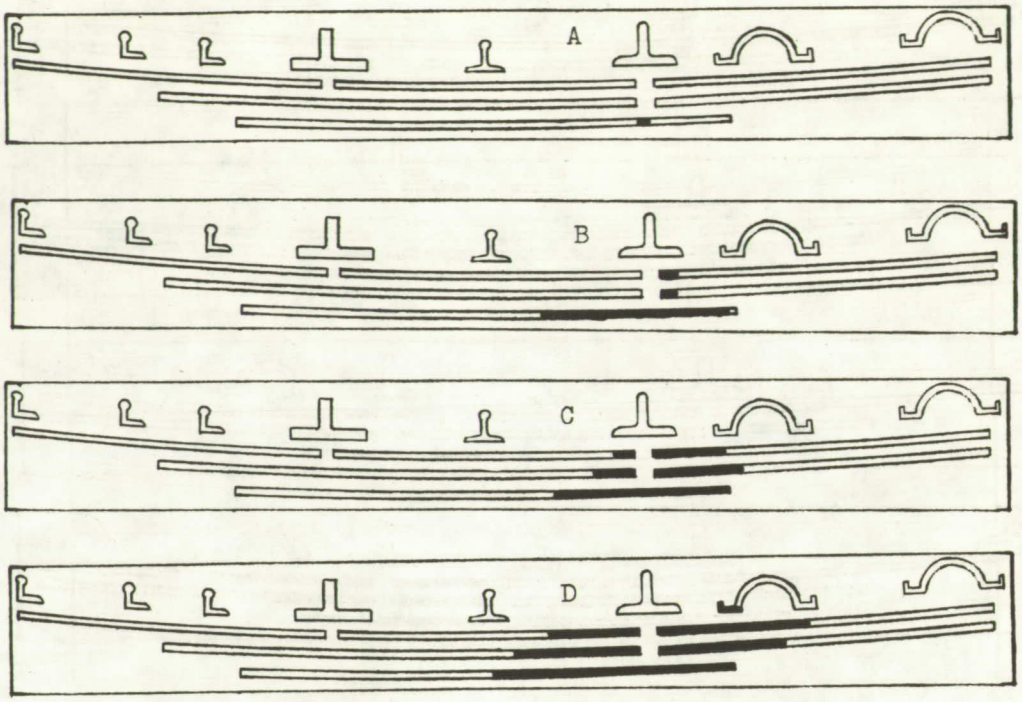

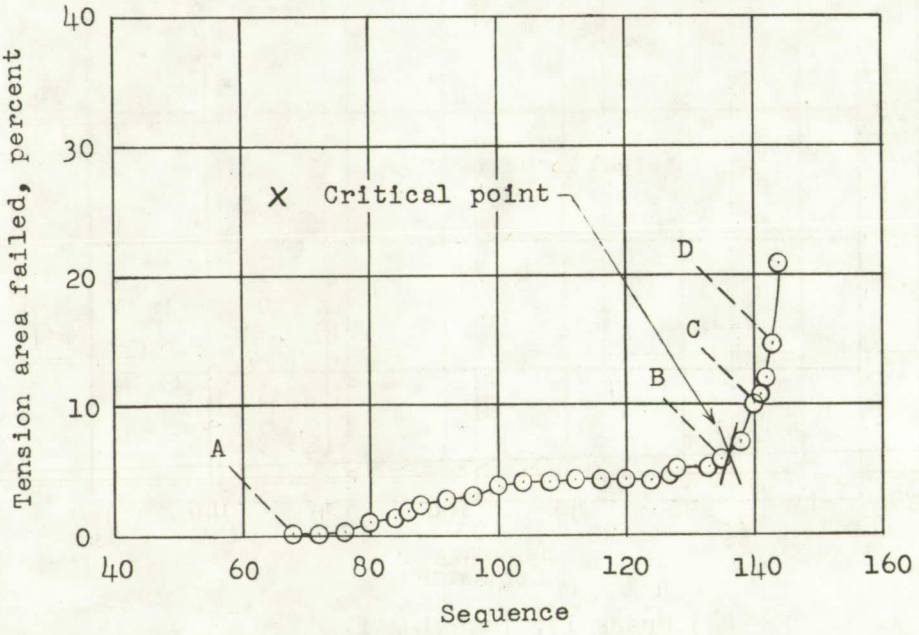

(b) Crack 11; location III.

Figure 6.- Continued.

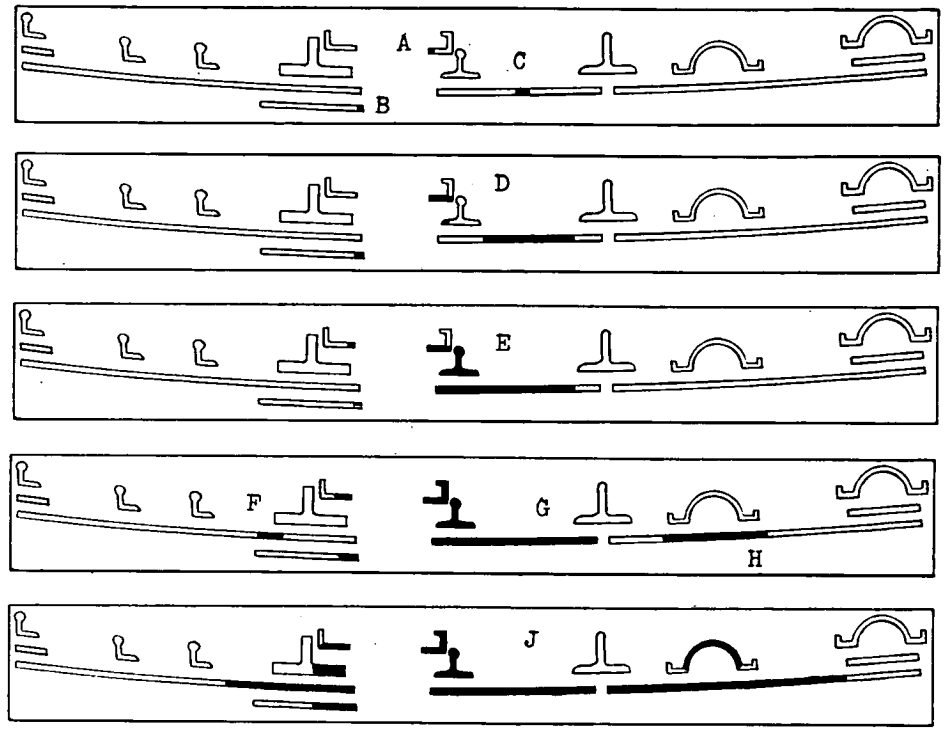

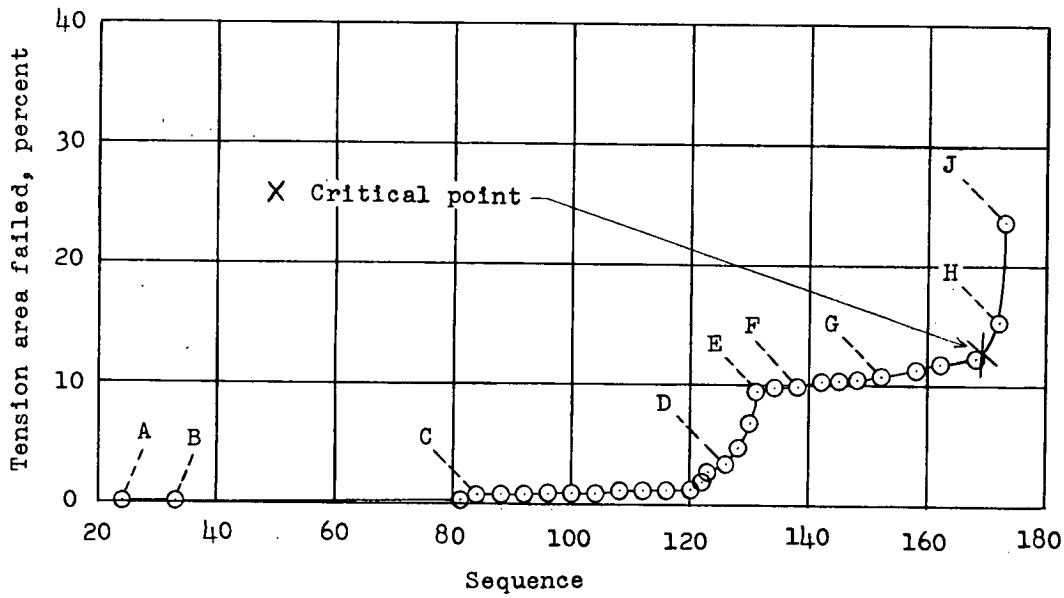

(c) Crack 17; location I.

Figure 6.- Continued.

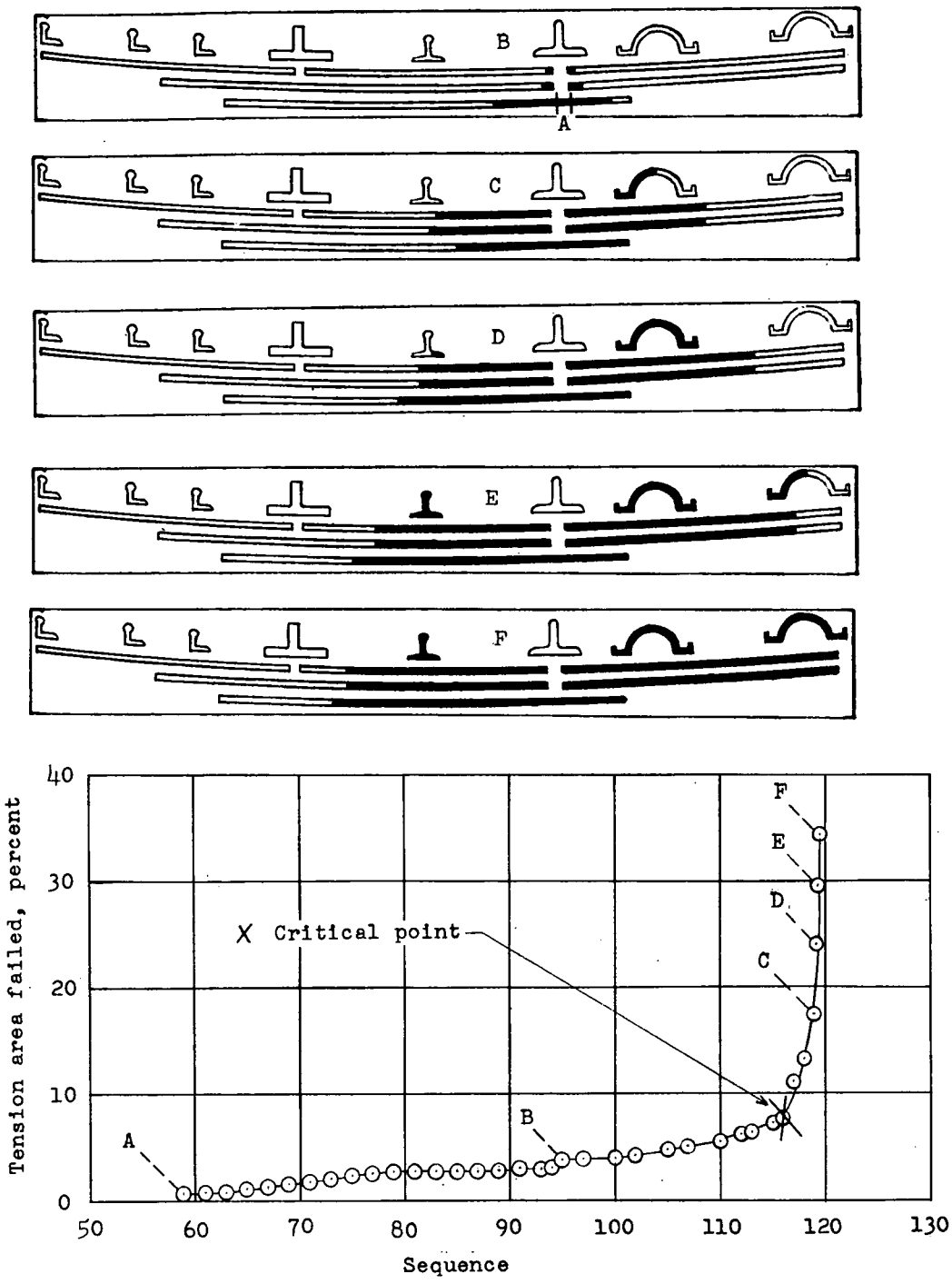

(d) Crack 20; location III.

Figure 6.- Continued.

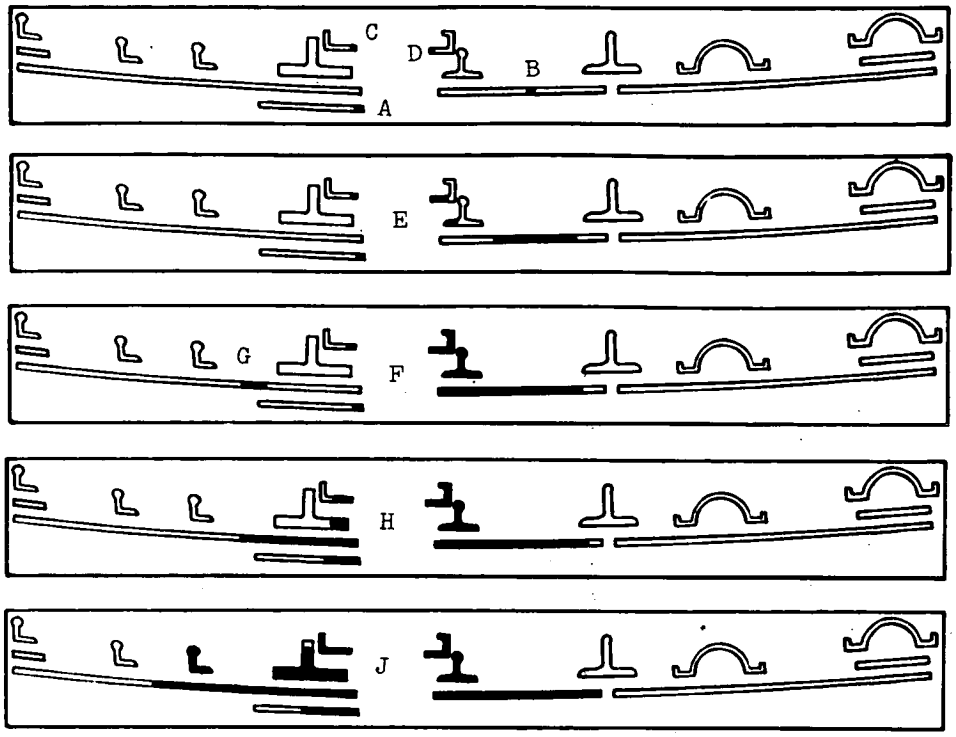

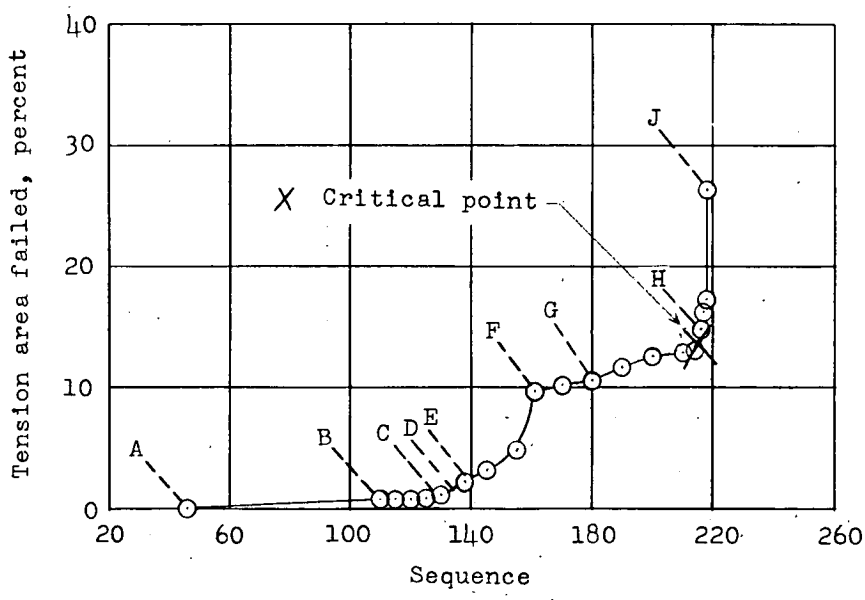

(e) Crack 33; location I.

Figure 6.- Continued.

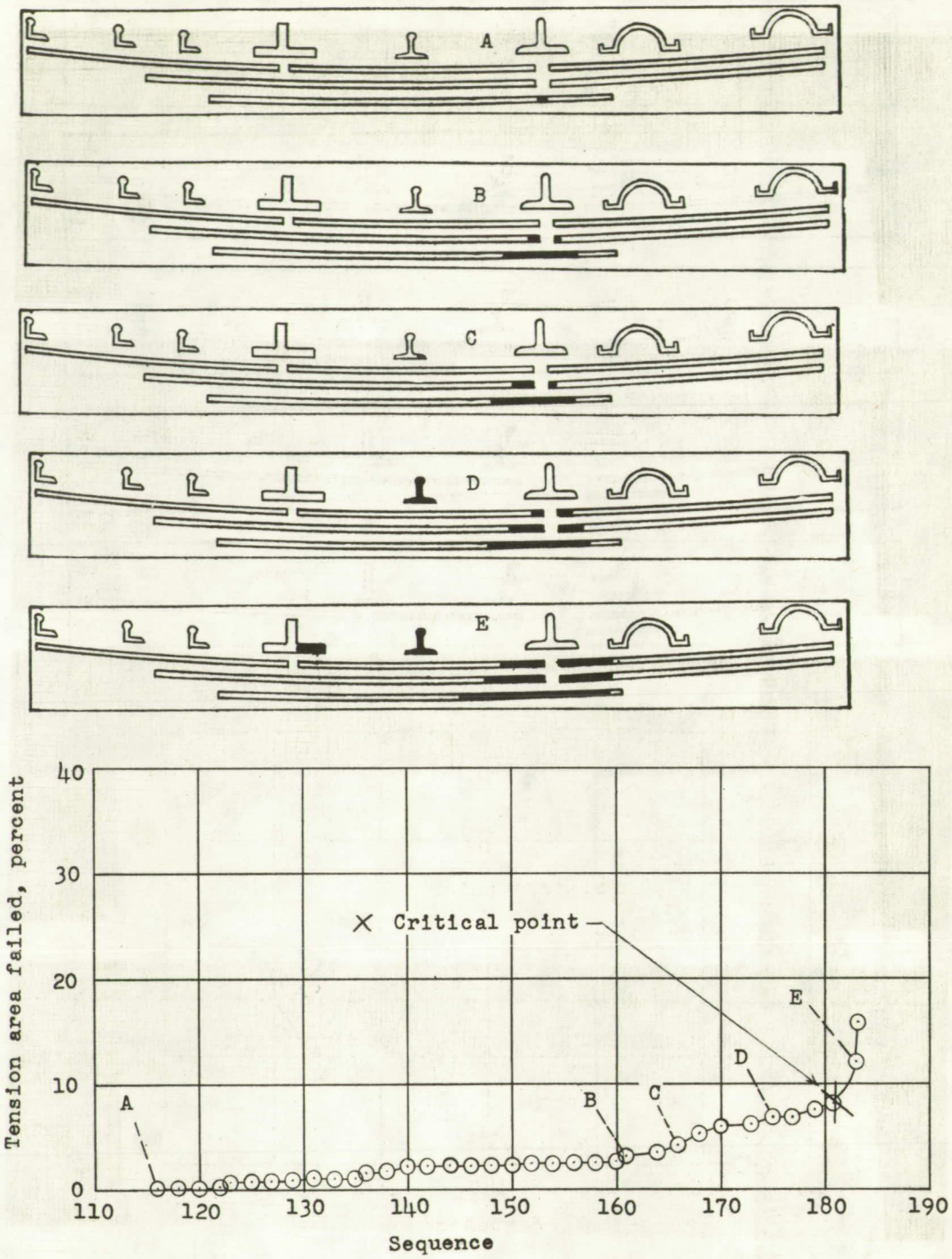

(f) Crack 41; location III.

Figure 6.- Concluded.

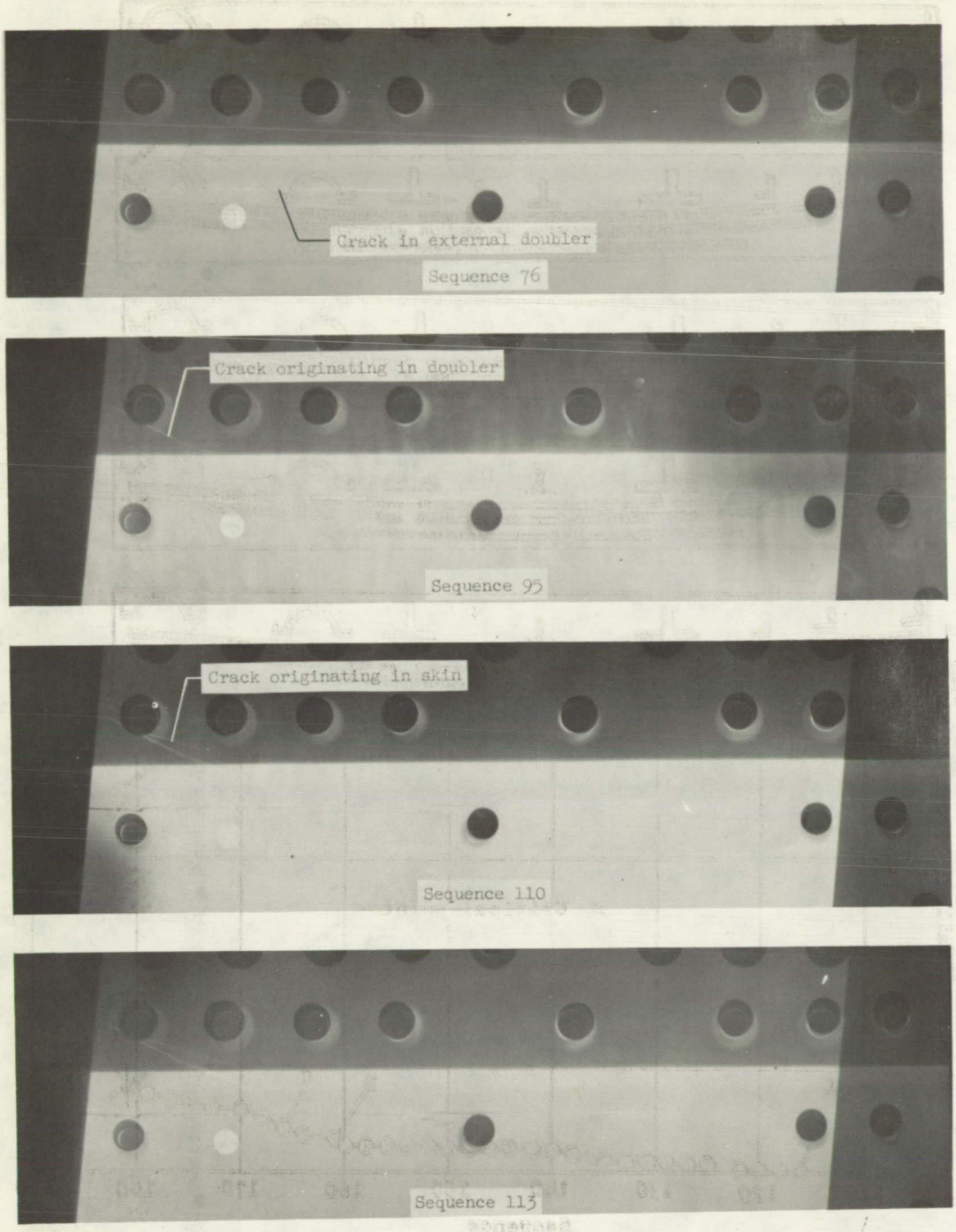

(a) Initial stages. L-57-2735

Figure 7.- X-ray photographs of crack 20 in joggle in external doubler plate.

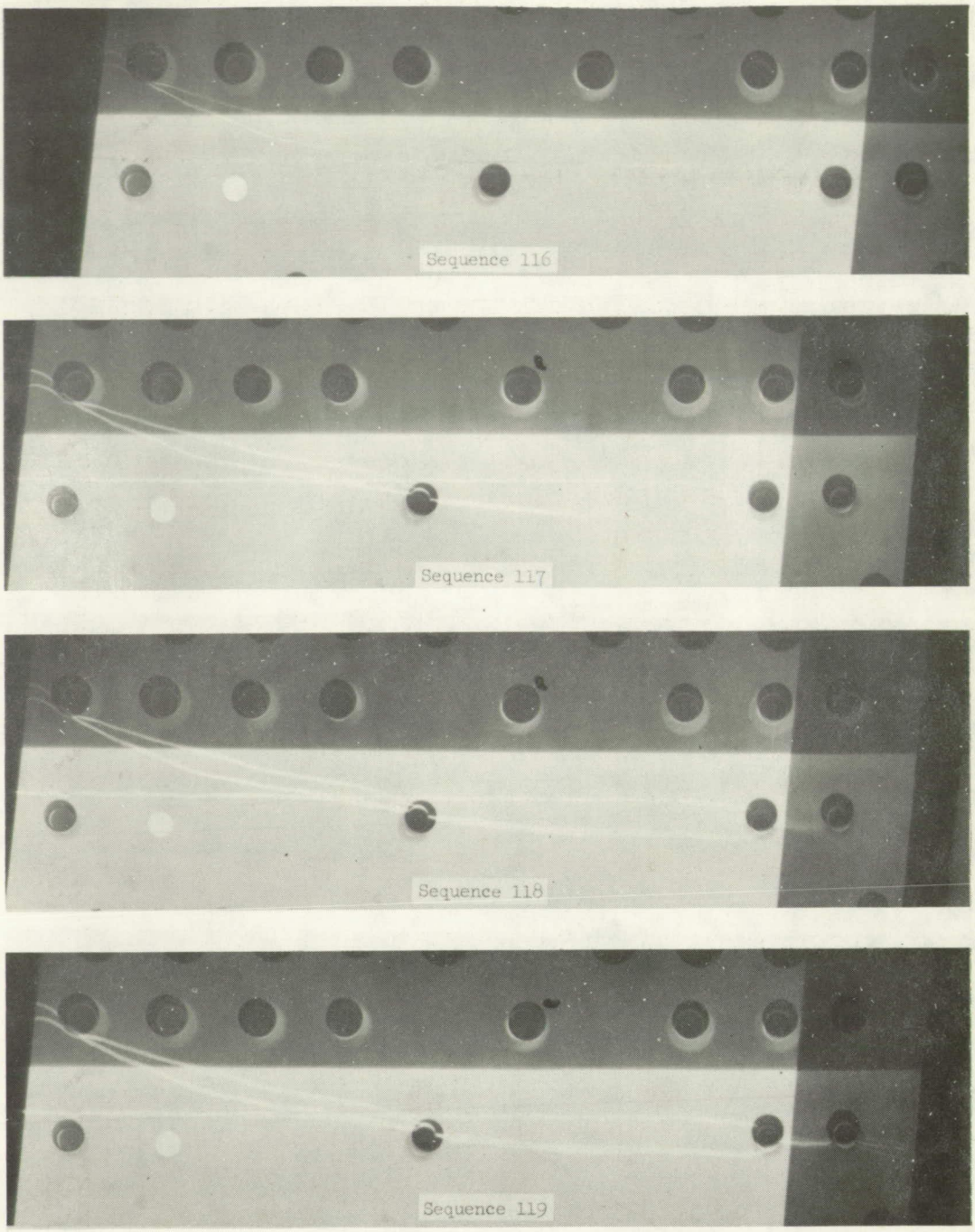

(b) Final stages. L-57-2736

Figure 7.- Concluded.

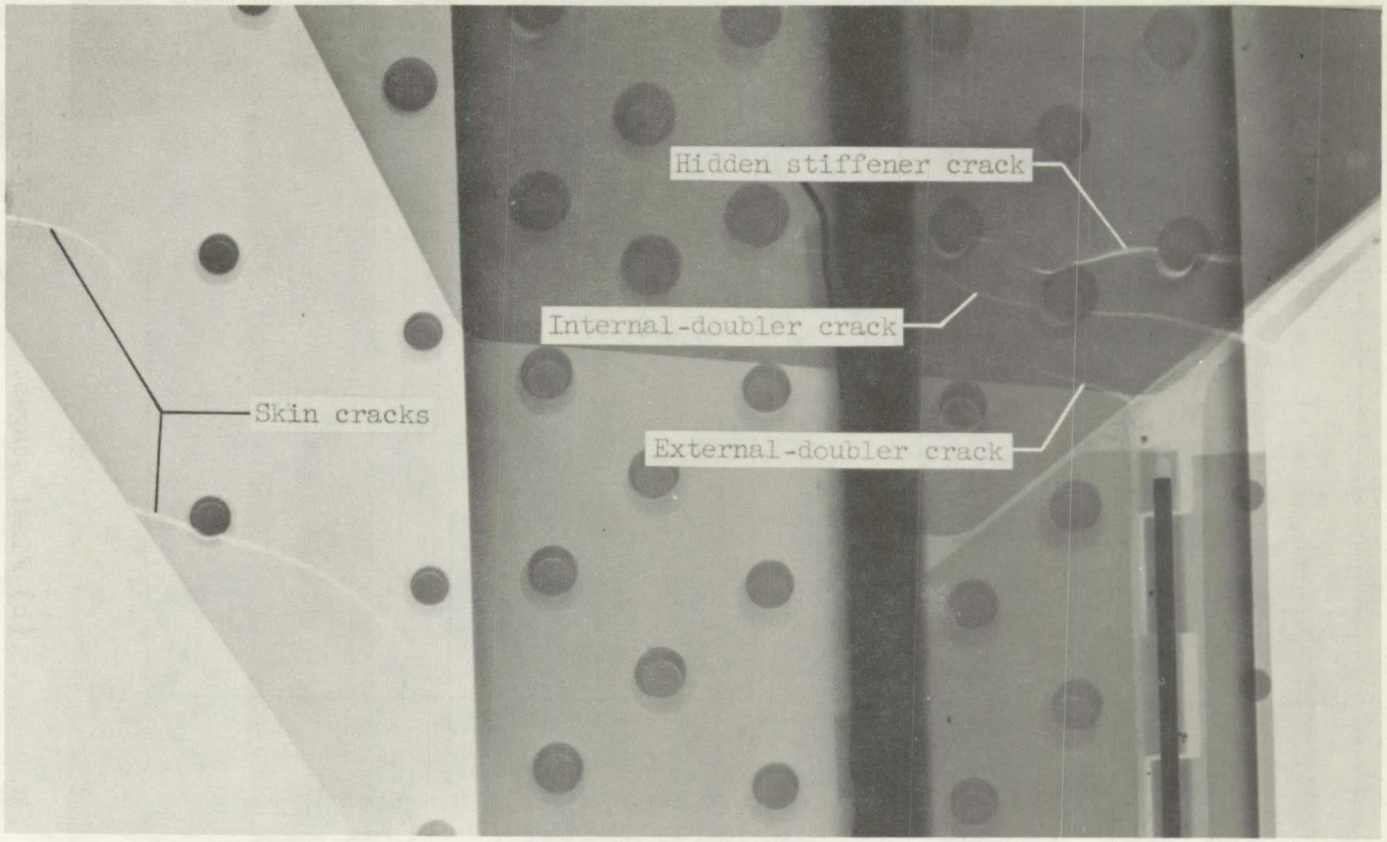

Figure 8.- X-ray photograph of crack in corner of inspection cutout. L-57-2737

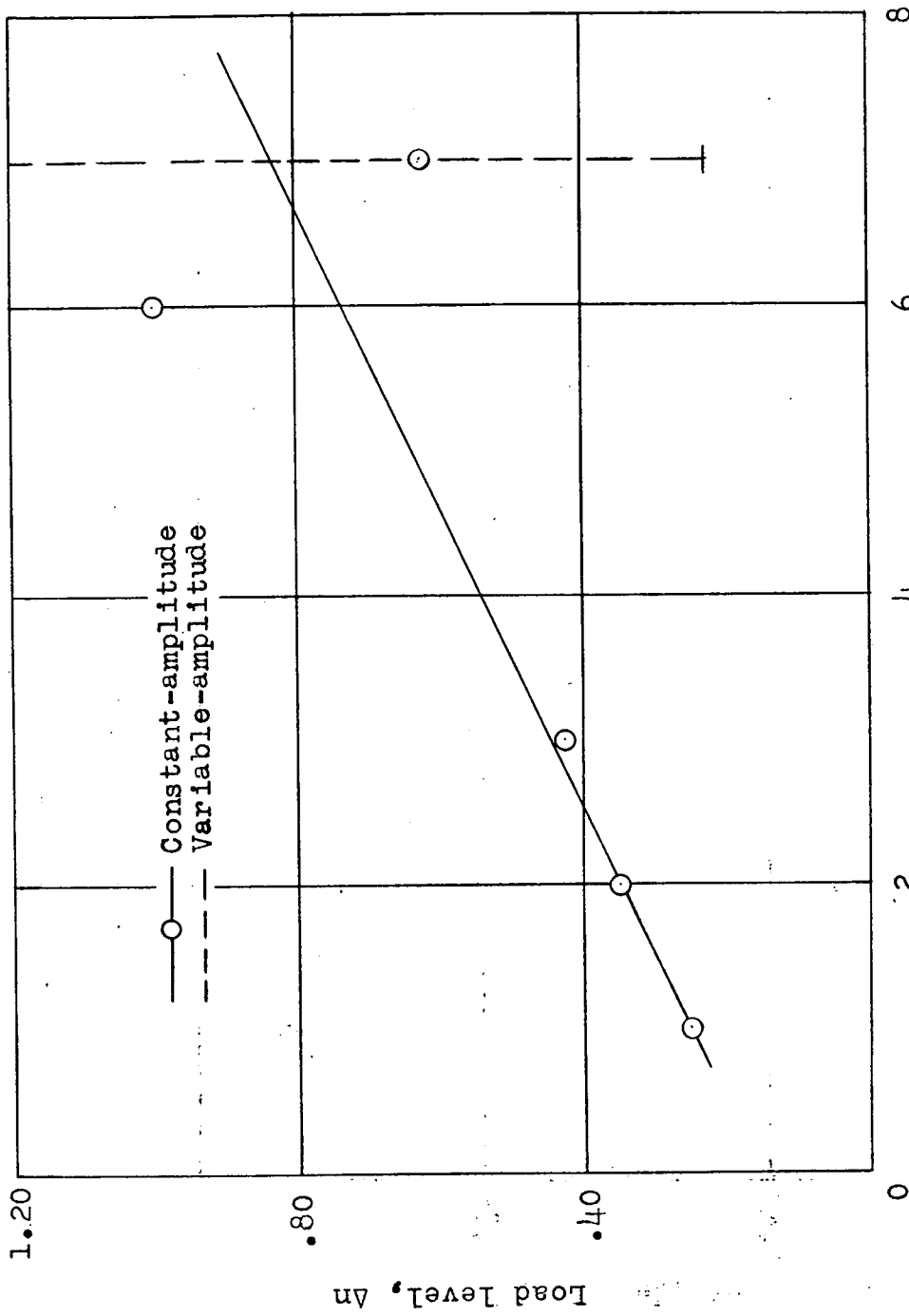

Figure 9.- Frequency of crack locations for constant-amplitude and variable-amplitude tests.

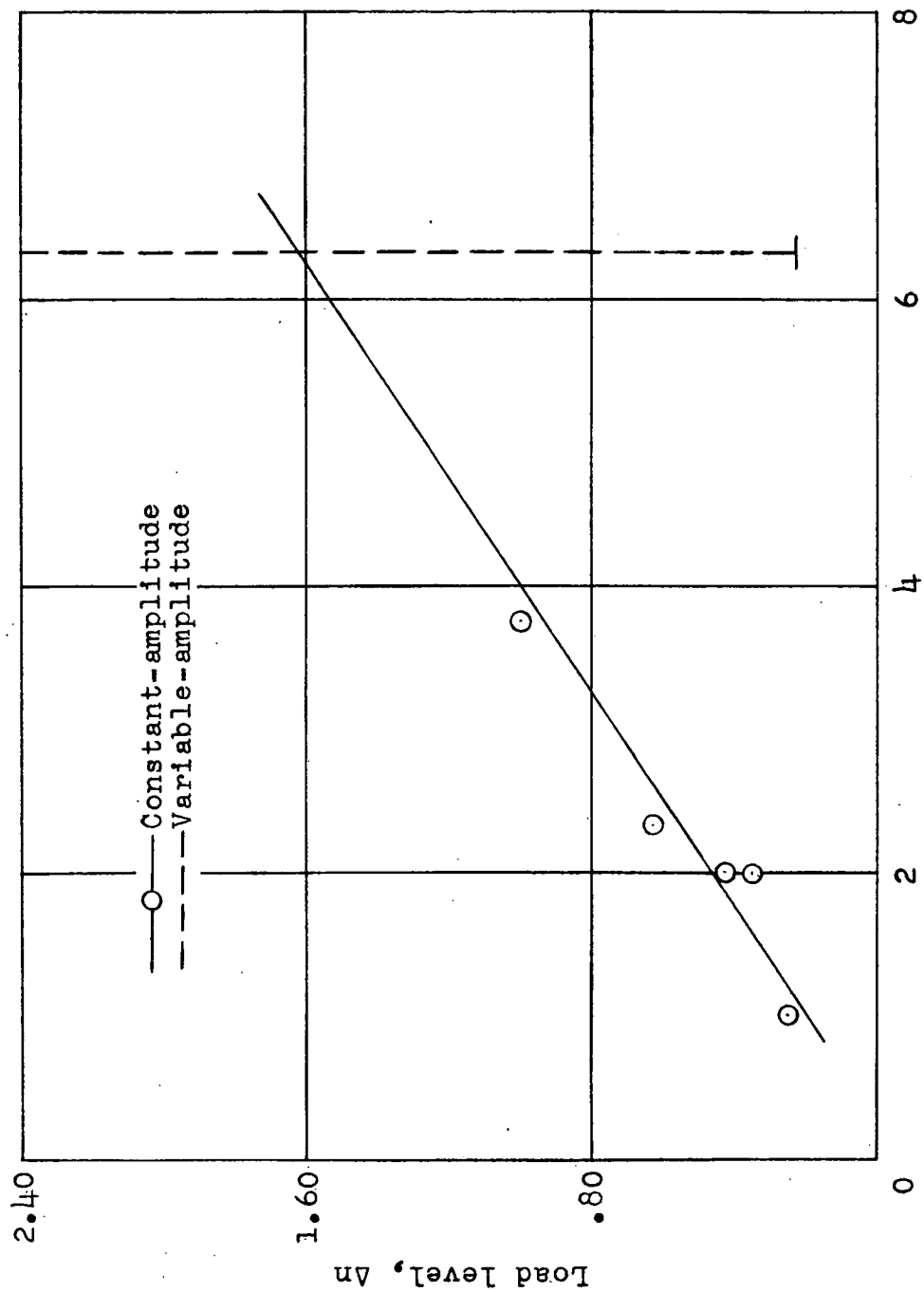

Figure 10.- Frequency of occurrence of cracks for constant-amplitude and variable-amplitude tests.

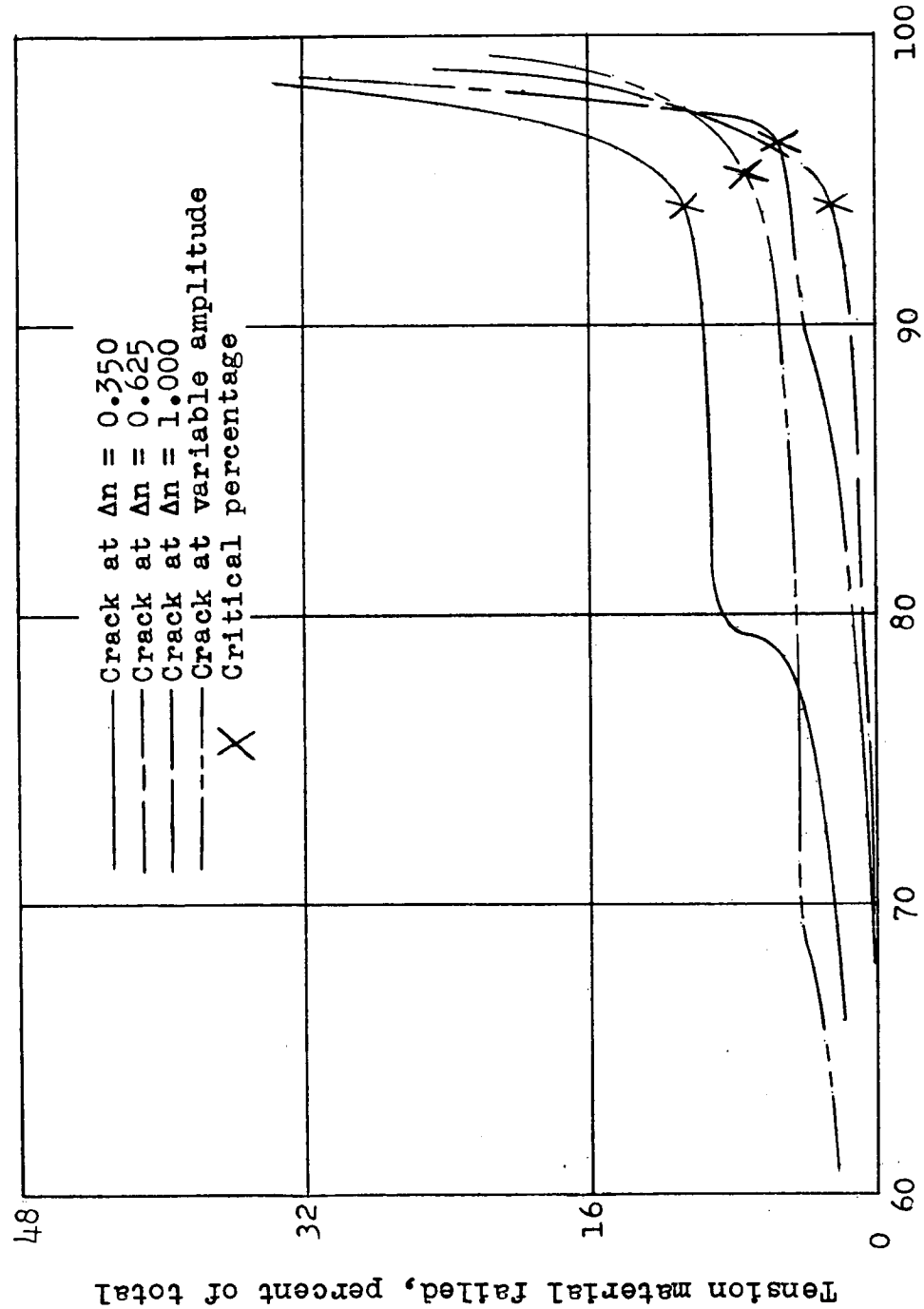

Figure 11.- Typical fatigue-crack propagation.

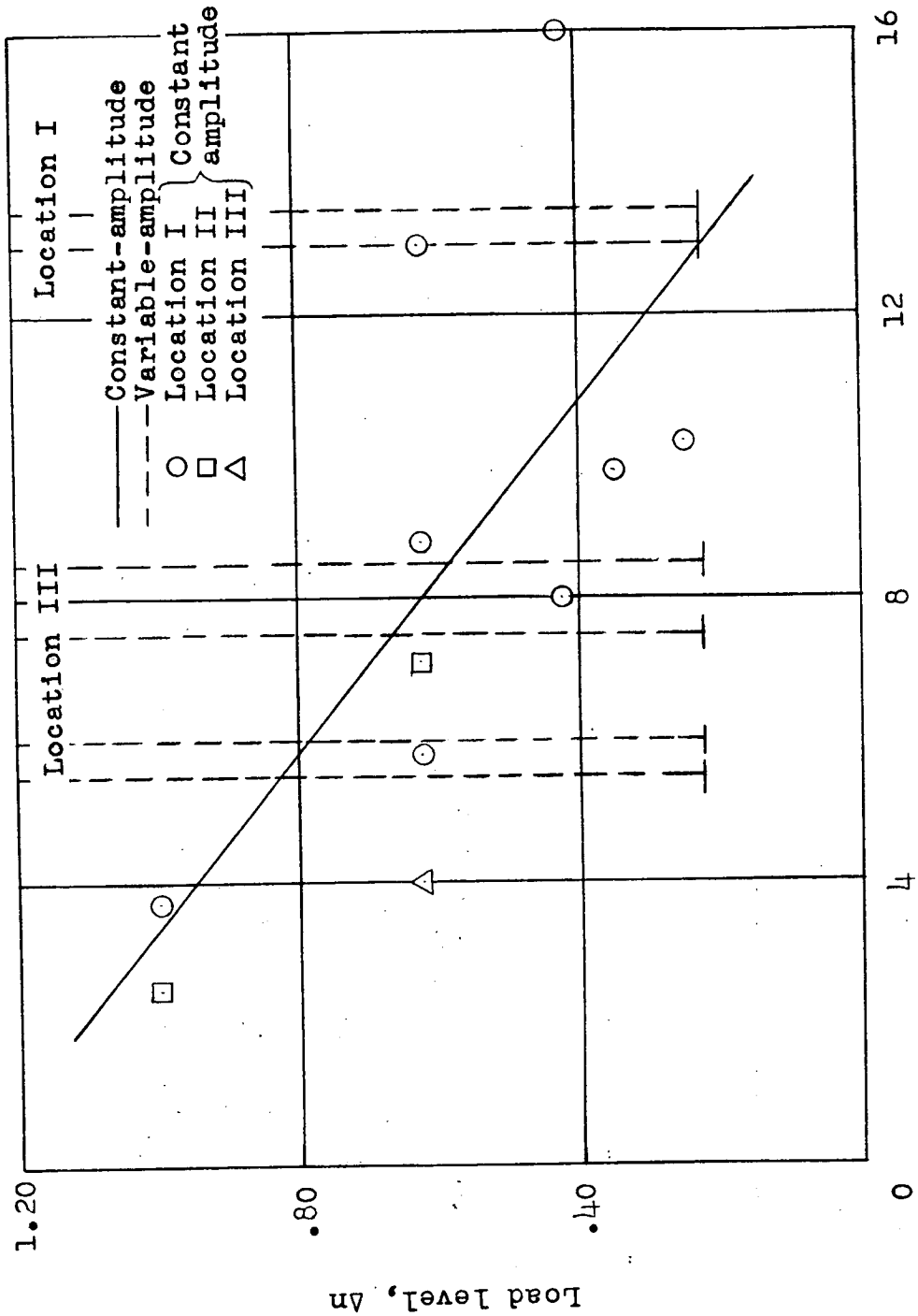

Figure 12.- Tension material failed at critical point.

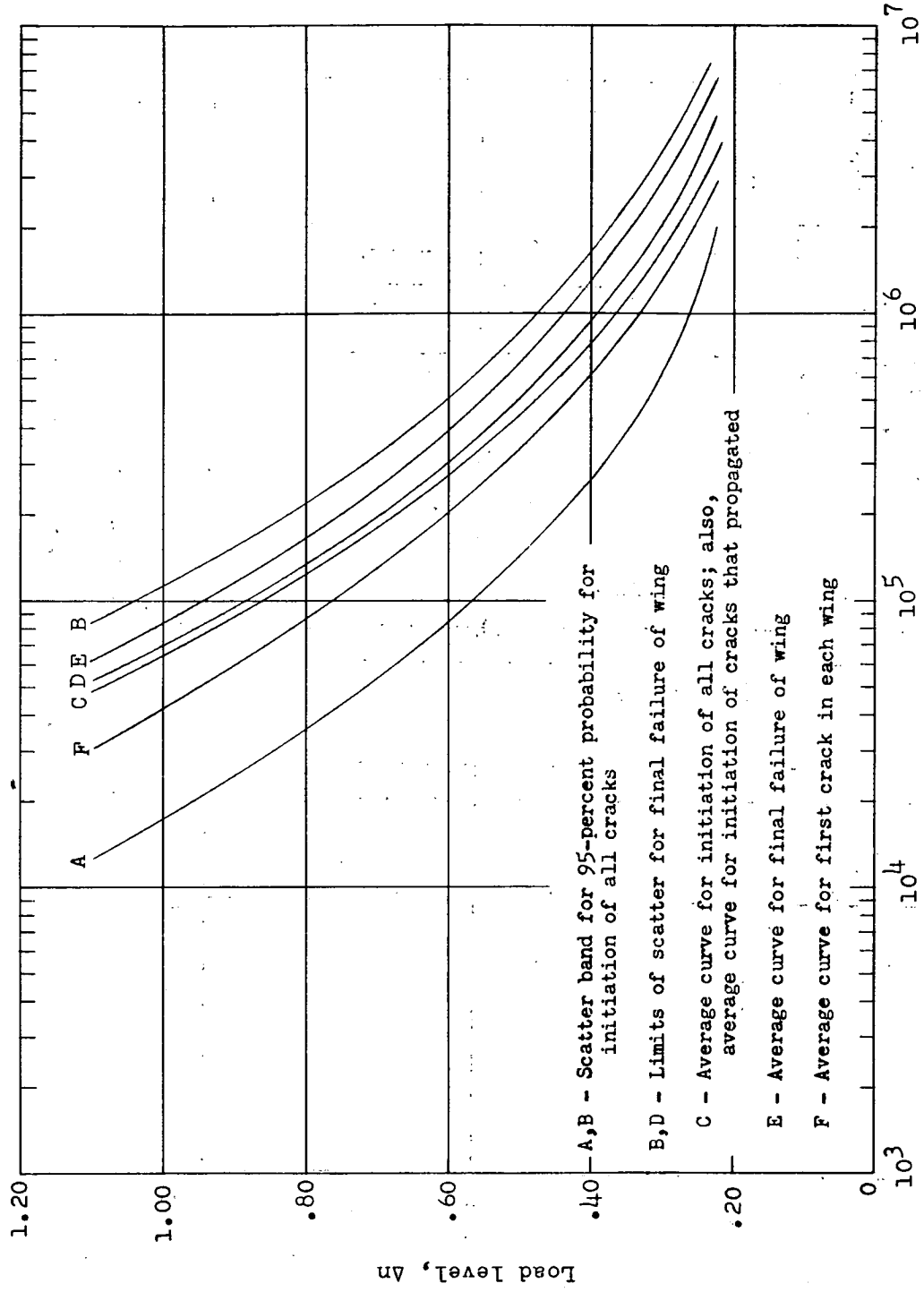

Figure 13.- Load-lifetime diagram from constant-amplitude tests.

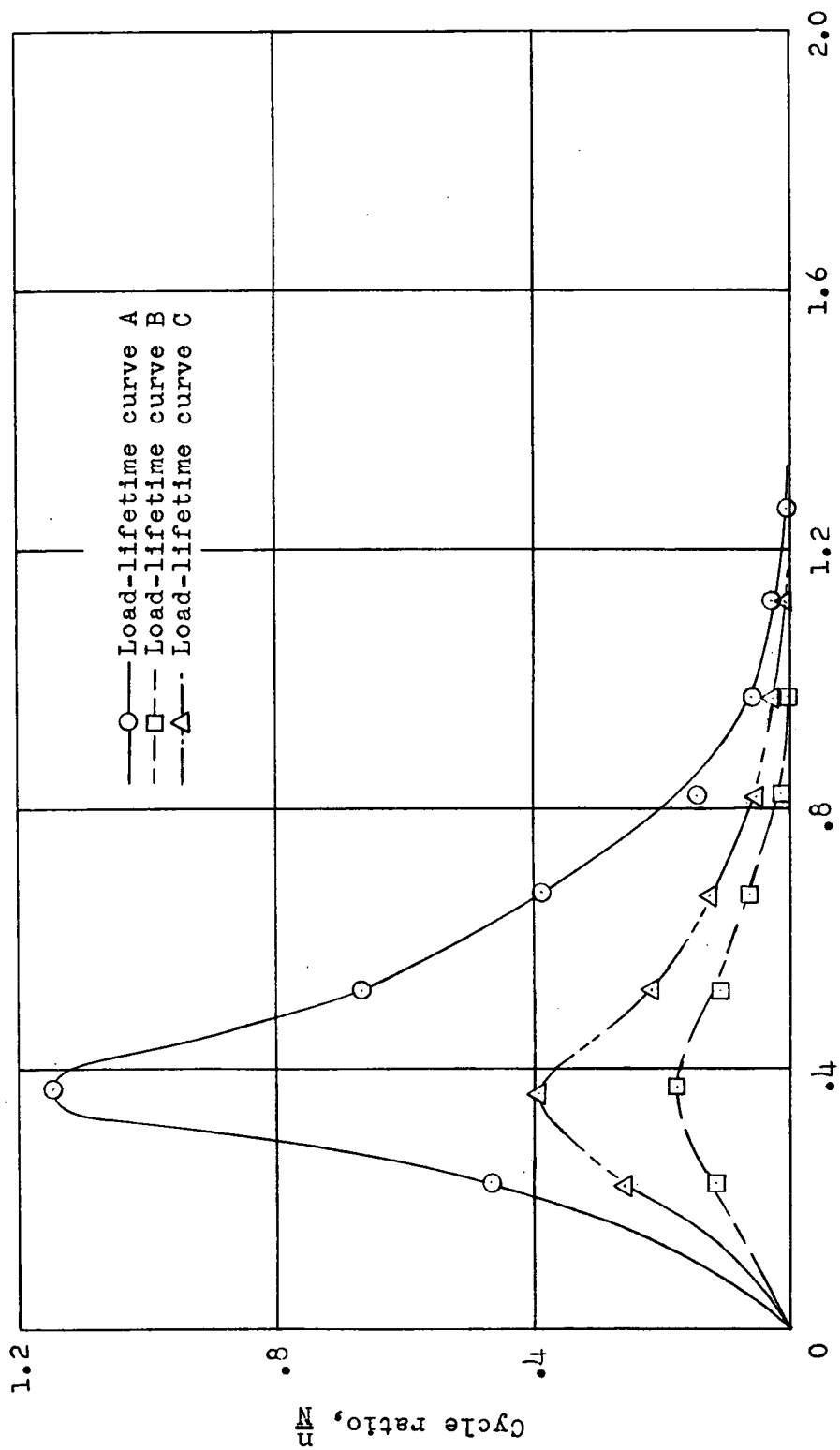

Figure 14.- Cycle ratios for crack 17, based on curves of figure 13.